

When to Match: A Cost-Balancing Principle for Dynamic Markets

Jie Liu

Department of Industrial Engineering & Decision Analytics, The Hong Kong University of Science and Technology, Clear Water Bay, Hong Kong S.A.R., China, iejiali@ust.hk

Hailun Zhang

School of Economics and Business Administration, Chongqing University, Chongqing, China, zhanghailun@cqu.edu.cn

Jiheng Zhang

Department of Industrial Engineering & Decision Analytics, The Hong Kong University of Science and Technology, Clear Water Bay, Hong Kong S.A.R., China, jiheng@ust.hk

Abstract. Matching platforms, from ridesharing to food delivery to competitive gaming, face a fundamental operational dilemma: match agents immediately to minimize waiting costs, or delay to exploit the efficiency gains of thicker markets. Yet computing optimal policies is generally intractable, sophisticated algorithms often rely on restrictive distributional assumptions, and common heuristics lack worst-case performance guarantees. We formulate a versatile framework for multi-sided matching with general state-dependent cost structures and non-stationary arrival dynamics. Central to our approach is a cost-balancing principle: match when accumulated waiting cost reaches a calibrated proportion of instantaneous matching cost. This equilibrium condition emerges from fluid-limit analysis and motivates a simple, adaptive Cost-Balancing (CB) algorithm requiring no distributional assumptions. We prove that CB achieves a competitive ratio of $(1 + \sqrt{\Gamma})$ under adversarial arrivals, where Γ quantifies economies of scale, guaranteeing cost within a constant factor of the offline optimum. In contrast, standard greedy and threshold policies can incur unbounded costs in adversarial scenarios. We further establish a universal lower bound of $(\sqrt{5} + 1)/2$ (the golden ratio), quantifying the fundamental price of uncertainty in online matching. Experiments on game matchmaking and real-world food delivery data demonstrate practical effectiveness, with CB consistently outperforming industry-standard heuristics.

Key words: dynamic matching; online algorithms; competitive analysis; matching markets

1. Introduction

Dynamic matching markets have become central to the modern service economy. From transportation and logistics to entertainment and healthcare, the efficient allocation of resources is no longer a static planning problem but a continuous, real-time control challenge. Platforms like Uber, Lyft, DoorDash, and competitive gaming servers operate in environments where supply and demand arrive stochastically, often with significant volatility. In these fast-paced markets, the platform's central algorithm acts as the market maker, bearing the responsibility of deciding not just who matches with whom, but when these matches occur (Uber 2023).

This temporal dimension introduces a fundamental operational trade-off. On the one hand, the need for responsiveness drives a preference for immediate matching. Delays lead to explicit waiting costs: idle drivers burn fuel, hungry customers grow impatient, and patients suffer. Excessive waiting also increases the risk

of abandonment, leading to lost revenue and market contraction. On the other hand, patience yields the benefit of market thickness. By strategically delaying decisions, a platform can aggregate a critical mass of agents, transforming a sparse, inefficient market into a dense, efficient one where economies of scale can be exploited. The magnitude of this trade-off varies across contexts, but its presence is universal in dynamic matching systems.

The business implications are substantial. In on-demand delivery, the difference between profitability and loss often hinges on the batch rate, i.e., the average number of orders a courier can deliver per trip. Immediate dispatch forces a one-to-one ratio, maximizing speed but crippling efficiency; batching can achieve higher ratios and reduce unit costs, but risks violating delivery guarantees and customer satisfaction. In the multi-billion-dollar e-sports industry, player retention is driven by the flow state achieved in well-matched games. An impatient algorithm that prioritizes short queues over skill parity creates unbalanced matches, where games are either too easy or too hard. Such mismatches are a leading cause of user churn, directly impacting platform revenue and growth. Thus, the matching policy is not merely a logistical tool. It is a strategic lever that directly impacts unit economics and long-term viability.

However, managing this trade-off is notoriously difficult because the future is unknown. The decision to wait is fundamentally a bet that future arrivals will offer matching quality that outweighs the accumulated cost of delay. In stable environments with predictable arrival patterns, this might be a calculated risk that can be optimized through standard stochastic control methods. But real-world platforms operate under highly non-stationary conditions: demand spikes unpredictably during rainstorms, driver supply fluctuates with traffic conditions, and player logins fluctuate significantly with time of day and promotional events. In such volatile environments, the optimal waiting window becomes a moving target that shifts continuously with changing market conditions. A static rule that works well on average, such as waiting a fixed two minutes, can be disastrous during a demand surge, leading to exploding queue lengths and system overload. Conversely, the same rule can be inefficient during a lull, causing unnecessary delays when immediate matching would be optimal.

Despite the practical significance of this problem, the existing toolkit for managing it remains divided between two extremes. On one side, industry practitioners often rely on ad hoc heuristics, such as fixed time windows (e.g., “batch every 30 seconds”) or simple queue-length thresholds. While operationally simple, these static rules lack theoretical robustness and struggle to adapt to the rapid, non-stationary shifts in demand intensity that characterize real-time platforms. When market conditions change, these heuristics require manual recalibration, creating operational overhead and introducing the risk of suboptimal performance during transition periods. On the other side, the academic literature offers sophisticated dynamic programming and stochastic control models. These approaches, while theoretically rigorous, typically depend on strong distributional assumptions (such as known Poisson arrival rates) or require complex state-dependent policies that are computationally brittle in volatile, real-world environments. Consequently, there is a distinct

lack of a unified framework that combines the operational simplicity of heuristics with the theoretical robustness of advanced online algorithms.

We bridge this gap by proposing a unified framework centered on a novel operational principle: Cost-Balancing (CB). Rather than optimizing for a specific, predicted future, we seek an operational equilibrium where the system self-regulates based on realized costs. Our core insight is that a matching decision should be triggered exactly when the accumulated cost of waiting reaches a calibrated proportion of the instantaneous cost of matching. This mechanism acts as an automatic control lever that adapts to changing market conditions. In low-demand periods, the system naturally waits longer to aggregate quality and exploit economies of scale. In high-demand spikes, the waiting costs accumulate faster, triggering quicker matches to prevent backlog and system overload. The algorithm’s decision boundary shifts dynamically with the state of the system, ensuring that matching occurs at the right moment regardless of whether the market is thick or thin. This intuition mirrors fundamental economic principles of marginal analysis but is applied here as a robust rule for real-time stochastic control that requires no distributional assumptions or parameter recalibration.

Our Contributions

Our work makes the following contributions to the theory and practice of dynamic matching:

1. We formulate a multi-sided matching model that captures general, state-dependent cost structures and non-stationary arrival dynamics, generalizing previous bipartite models to accommodate applications such as ride-pooling, team formation, and multi-resource allocation. Building on this framework, we introduce the Cost-Balancing algorithm, a simple, adaptive policy that implements our equilibrium principle without requiring distributional information or extensive parameter tuning, making it immediately deployable in practice.
2. We characterize the structural properties of the optimal policy. We prove that while the general problem is intractable, a relaxed model with Poisson arrivals and a convex, supermodular matching cost function admits an optimal policy with a monotone threshold structure. Grounding our approach in fluid-limit analysis of this relaxed model, we uncover the fundamental equilibrium principle that motivates cost-balancing.
3. We prove that the CB algorithm achieves a competitive ratio of $(1 + \sqrt{\Gamma})$ under adversarial arrivals, where Γ quantifies the economies of scale in the matching cost function. This robust guarantee contrasts sharply with standard heuristics: greedy and fixed-threshold policies can incur unbounded costs in worst-case scenarios. We further establish a universal lower bound of $(\sqrt{5} + 1)/2$ (the golden ratio) on the competitive ratio for any online algorithm, characterizing the unavoidable “price of uncertainty” in dynamic matching and demonstrating that our algorithm’s performance is within a modest factor of the theoretical optimum.
4. We analyze the general attribute-based matching model where matching costs depend on specific agent attributes rather than aggregate queue lengths. We prove that computing optimal policies is NP-hard for multi-sided markets with three or more agent types, and establish that no online algorithm can

achieve bounded competitive ratios when the adversary controls both arrival times and agent attributes. These impossibility results characterize the fundamental barriers of attribute-based models and motivate the queue-based abstraction as a tractable alternative that enables robust performance guarantees.

5. We demonstrate the algorithm’s practical effectiveness through extensive experiments on game matchmaking and real-world food delivery data. A key advantage of our approach is its self-tuning nature: unlike threshold policies that require constant recalibration as demand shifts, the CB mechanism adapts automatically. Our algorithm consistently outperforms industry-standard batching heuristics across diverse market conditions.

The remainder of the paper is organized as follows. Section 2 reviews the related literature, positioning our work within three research streams. Section 3 formally defines the multi-sided matching model, introduces the Cost-Balancing algorithm, and states our main result on competitive ratio guarantees. Section 4 develops the theoretical foundation by analyzing the structure of optimal policies in a relaxed model, revealing the intuition underlying the Cost-Balancing algorithm through fluid limit analysis. Section 5 presents the competitive ratio analysis of the Cost-Balancing algorithm and demonstrates the fragility of standard benchmark policies, as well as the unavoidable price of uncertainty in dynamic matching. Section 6 characterizes the fundamental computational and information-theoretic barriers of the general attribute-based model, clarifying the role of the queue-based abstraction. Section 7 validates the algorithm through numerical experiments on game matchmaking and food delivery data, demonstrating practical effectiveness across diverse market conditions. Finally, Section 8 concludes the paper and suggests directions for future research.

2. Literature Review

Dynamic matching has emerged as an important research domain bridging operations research, algorithmic economics, and theoretical computer science. This paper proposes a cost-balancing mechanism that formalizes the temporal equilibrium between immediate matching costs and the opportunity cost of delay. Our contribution engages with three literature streams: (1) competitive ratio analysis of online matching algorithms, (2) the matching-waiting trade-off in operations, and (3) the effectiveness of simple mechanisms in complex environments.

2.1. Competitive Ratio Analysis

The theoretical computer science community has pioneered competitive ratio analysis for online bipartite matching. The seminal work of Karp et al. (1990) established a competitive ratio of $1 - \frac{1}{e}$ for adversarial arrivals, spawning two key extensions: stochastic arrival models (Feldman et al. 2009, Bahmani and Kapralov 2010, Manshadi et al. 2012, Jaillet and Lu 2014) that derive improved ratios under distributional assumptions, and stochastic reward frameworks (Mehta and Panigrahi 2012, Huang and Zhang 2020, Goyal and Udwani 2023) that extend the analysis to uncertain match values; see Mehta et al. (2013) for a comprehensive survey. Our work contributes a constant-competitive algorithm to this literature that requires no distributional assumptions and generalizes beyond bipartite to multi-sided matching.

2.2. The Matching-Waiting Trade-off

A central challenge in dynamic matching systems, extensively studied within the operations research community, lies in balancing the immediate rewards of matching against the long-term optimization potential afforded by waiting. Our modeling framework is closely related to the matching queues literature (Gurvich and Ward 2015, Afeche et al. 2022). Gurvich and Ward (2015) analyze the dynamic control of matching queues to minimize holding costs, and Afeche et al. (2022) explore the optimal design of matching topologies to balance rewards and delays.

The contemporary literature formalizes this trade-off through distinct optimization frameworks. Multi-stage optimization approaches, such as those in Feng et al. (2024) and Feng and Niazadeh (2025), achieve competitive vertex-weighted matching by dynamically transitioning between greedy and hedging strategies. A complementary line of work (Wei et al. 2023, Kerimov et al. 2024, 2025, Chen et al. 2025b) adopts regret minimization to benchmark policies against optimal hindsight decisions, often in settings with heterogeneous demand and supply.

Platform-specific dynamics further shape this trade-off, particularly in spatial settings where physical constraints impose unique challenges. Kanoria (2025) characterize the scaling behavior of achievable costs in dynamic spatial matching with uncertain locations. In ride-sharing, Ashlagi et al. (2019) and Aouad and Saritaç (2022) incorporate stochastic abandonment and heterogeneous sojourn times, while Wang et al. (2024) model abandonment and cancellation dynamics, and Liang et al. (2025) derive exact cost formulas for spatial matching on a circle. In on-demand delivery, Gautam and Geunes (2024) propose a cost-based threshold policy for delivery dispatch, while Chen and Hu (2024) and Ma et al. (2025) focus on delay-sensitive dispatching and spatial pooling, respectively. More broadly, the link between market thickness and matching quality has been explored across various platform contexts (Ashlagi and Roth 2021, Chen et al. 2025a, Immorlica et al. 2023, Keskin et al. 2024, Zhao et al. 2024), with Kohlenberg and Gurvich (2025) specifically quantifying the “cost of impatience” via scaling laws.

A related stream of literature investigates the mechanics of batching and delayed decisions. Xie et al. (2025) and Wei et al. (2021) study the benefits of batching in online matching, and Bhimaraju et al. (2026) examine optimal batching schedules with competitive guarantees. Our work differs from these contributions by proposing a unified, cost-centric principle rather than a parametric or application-specific solution, and extends to a broader class of multi-sided matching problems.

2.3. The Effectiveness of Simple Policies

A growing body of literature in economics and operations management demonstrates that simple heuristic policies can achieve near-optimal performance in dynamic matching markets (Akbarpour et al. 2020, Baccara et al. 2020, Mertikopoulos et al. 2024, Loertscher et al. 2022, Ashlagi et al. 2023). Particularly relevant is Mertikopoulos et al. (2024), who study the dynamic clearing game in two-sided markets with Poisson arrivals and characterize the conditions under which simple policies are optimal.

Subsequent research explores various simple heuristics across different settings. [Blanchet et al. \(2022\)](#) analyze departure-based threshold policies under general random utilities, while [Balkanski et al. \(2023\)](#) and [Gupta \(2024\)](#) establish performance bounds for greedy algorithms on specific graph structures. [Eom and Toriello \(2025\)](#) show that simple batching policies achieve near-optimal performance even with impatient agents. [Kerimov et al. \(2024\)](#) introduce the “general position gap” to characterize when periodic clearing approximates optimal values in multiway matching, and their follow-up work ([Kerimov et al. 2025](#)) proves that greedy heuristics can be hindsight optimal in two-way settings. [Ma et al. \(2025\)](#) propose a potential-based heuristic for delivery pooling under specific reward structures.

A common thread in this literature is the reliance on stochastic assumptions to establish performance guarantees. Our Cost-Balancing algorithm achieves provable competitive guarantees under adversarial arrivals without distributional requirements or asymptotic market conditions. Despite its simple design, our policy consistently outperforms standard benchmark heuristics in both theoretical worst-case analysis and empirical experiments, highlighting its robustness and practical value.

3. Model, Algorithm, and Main Results

In this section, we develop a general framework for multi-sided matching that captures the essential structural elements of these markets: stochastic arrivals, the cost of waiting, and the economies of scale inherent in matching. This section formalizes the problem environment, introduces the Cost-Balancing algorithm as a robust solution mechanism, and states our main performance guarantee.

3.1. The Multi-sided Matching Problem

We consider a continuous-time matching system with $N \geq 2$ distinct types of agents.¹ Agents of each type $i \in \{1, \dots, N\}$ arrive dynamically over time and must be matched into complete N -tuples (one agent from each type) to complete service. Let $A_i(t)$ denote the counting process of type- i arrivals by time t , with arrival epochs $\{\sigma_{i,k}\}_{k \geq 1}$ defined by $\sigma_{i,0} = 0$ and $\sigma_{i,k} = \inf\{t : A_i(t) \geq k\}$ for $k \geq 1$. We impose no distributional assumptions on these arrival streams: they may be deterministic, stochastic, or non-stationary, and are assumed only to be non-explosive (i.e., finitely many arrivals in any finite interval). This generality allows our framework to accommodate the volatile and potentially adversarial arrival patterns characteristic of real-world platforms.

The state of the system at time $t \geq 0$ is captured by the vector of queue lengths $\mathbf{X}(t) = (X_1(t), \dots, X_N(t)) \in \mathbb{Z}_+^N$, where $X_i(t)$ denotes the number of unmatched type- i agents. A matching decision is feasible at time t if and only if $\min_j X_j(t) \geq 1$, i.e., at least one agent of each type is available. The controller makes matching decisions at arrival epochs. Upon arrival of a type- i agent at time t , the queue length X_i increases instantaneously by one, and the controller observes the post-arrival state $\mathbf{X}^+(t) = \mathbf{X}(t^-) + \mathbf{e}_i$, where \mathbf{e}_i is the

¹ When $N = 1$, we assume a match consists of a pair formed by two agents of the same type.

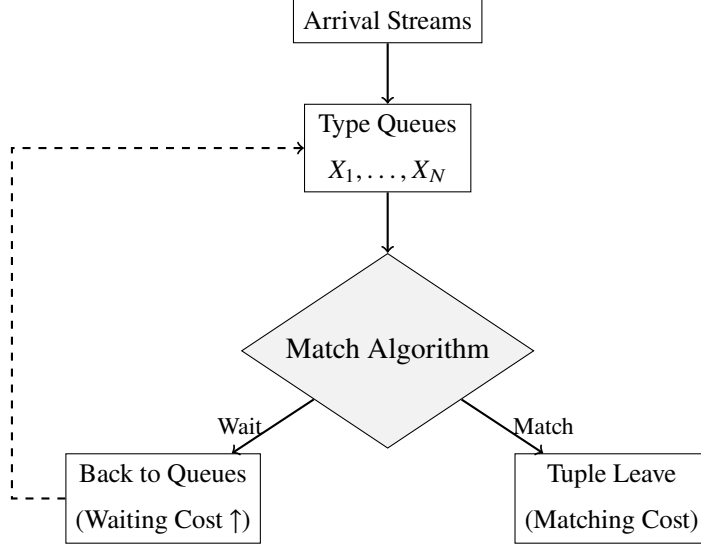


Figure 1 System Dynamics and Decision Flow

i -th standard basis vector. The controller then decides whether to execute a match. If a match is executed, one agent from each type is selected to form an N -tuple that exits the system, and the state transitions to $\mathbf{X}(t) = \mathbf{X}(t^-) + \mathbf{e}_i - \mathbf{1}$, where $\mathbf{1} = (1, \dots, 1)^\top \in \mathbb{Z}_+^N$. If no match is executed, the state remains at $\mathbf{X}(t) = \mathbf{X}^+(t)$.

Each executed match incurs a state-dependent cost $f(\mathbf{X}^+(t))$, where $f : \mathbb{Z}_+^N \rightarrow \mathbb{R}_+$ represents the minimum cost of forming a matched tuple given the current pool of available agents. This cost captures factors such as geographic dispersion in ride-sharing, skill disparity in gaming, or delivery distance in logistics. We impose the following structural assumption on the matching cost function.

ASSUMPTION 1. *The matching cost incurred at time t is a function $f(\cdot)$, which depends on $\{X_i(t), 1 \leq i \leq N\}$, the number of unmatched agents at time t for each type. Furthermore, $f(\cdot)$ satisfies the monotonicity property, i.e., $f(\mathbf{x}) \leq f(\mathbf{y})$ whenever $\mathbf{x} \succeq \mathbf{y}$.²*

Assumption 1 is assumed throughout the paper except Section 6; it captures the market thickness effect: as the pool of available agents grows, the platform can select better matches, thereby reducing matching costs. This property arises naturally in many applications. In ride-sharing, larger driver pools enable better geographic clustering; in gaming, more players allow tighter skill matching; in delivery, more orders permit efficient route bundling. We adopt a queue-dependent cost structure rather than modeling individual agent attributes explicitly. This modeling choice is both practically motivated and theoretically necessary. In practice, queue length serves as a sufficient statistic that aggregates the benefit of agent heterogeneity. Theoretically, we show in Section 6 that the general attribute-based model faces fundamental barriers: computing optimal policies is NP-hard even in static settings, and no online algorithm can achieve a bounded

² Here $\mathbf{x} \succeq \mathbf{y}$ means $\mathbf{x}[i] \geq \mathbf{y}[i]$ for each i , where $\mathbf{x}[i]$ ($\mathbf{y}[i]$) is the i -th component of \mathbf{x} (\mathbf{y}).

competitive ratio under adversarial attribute arrivals. These results motivate Assumption 1 as a tractable abstraction that enables meaningful performance guarantees.

Unmatched agents incur waiting costs while residing in their respective queues. We assume a linear waiting cost structure: each unmatched type- i agent incurs a cost at rate $c_i > 0$ per unit time. The instantaneous waiting cost rate of the system is defined as

$$w(\mathbf{X}(t)) := \sum_{i=1}^N c_i X_i(t),$$

representing the aggregate cost rate across all waiting agents. The waiting cost parameters $\{c_i\}$ may differ across types, reflecting heterogeneous time-sensitivity (e.g., passengers may be more impatient than drivers).

A policy π specifies, at each arrival epoch, whether to execute a match based on the current system state. The total cost under policy π over a horizon $[0, T]$ consists of cumulative waiting costs and matching costs:

$$J_T^\pi := \int_0^T w(\mathbf{X}(t)) dt + \sum_{k=1}^{M(T)} f(\mathbf{X}^+(\tau_k)),$$

where $M(T)$ denotes the number of matches executed by time T , and τ_k is the epoch of the k -th match. When arrivals terminate at a finite time T , we take J_T^π as our performance measure. For infinite-horizon problems, we consider the long-run average cost:

$$J^\pi := \limsup_{T \rightarrow \infty} \frac{1}{T} J_T^\pi.$$

The platform's objective is to find a policy π^* that minimizes this cost. In the later analysis, we omit the subscript T for simplicity and denote the objective value by J^π for any policy π and problem instance.

3.2. The Cost-Balancing Algorithm

Standard approaches to this problem typically fall into two categories: static policies that rely on fixed parameters (e.g., matching every 5 minutes or when the queue reaches a threshold of 10), and dynamic approaches that require precise knowledge of future arrival rates. Both approaches suffer from significant drawbacks in volatile environments. Static policies fail to adapt to demand surges, while dynamic policies are sensitive to estimation errors in arrival rate forecasts. To overcome these limitations, we introduce the Cost-Balancing algorithm, presented in Algorithm 1.

The CB algorithm operates on a simple but powerful principle: trigger a match when the accumulated waiting cost becomes comparable to the instantaneous matching cost. Specifically, the algorithm continuously tracks the cumulative waiting cost W incurred since the last match. At each arrival epoch, if matching is feasible, the algorithm checks whether the current matching cost $M = f(\mathbf{x})$ satisfies the condition $M \leq \alpha W$, where $\alpha > 0$ is a tuning parameter. When this condition holds, a match is executed and the waiting cost counter resets to zero.

Algorithm 1 Cost-Balancing Algorithm

Require: Arrival streams for each type $i \in \{1, \dots, N\}$; balancing parameter $\alpha > 0$.

Ensure: Total cost $J = \text{Total waiting cost} + \text{Total matching cost}$

```

1: Initialize  $\mathbf{x} \leftarrow \mathbf{0}$                                 ▷ State vector:  $x_i = \text{pending arrivals of type } i$ 
2:  $W \leftarrow 0$                                          ▷ Accumulated waiting cost since last matching
3:  $J \leftarrow 0$                                          ▷ Total system cost
4: while arrival streams not exhausted or  $\mathbf{x} \neq \mathbf{0}$  do
5:   Process new arrivals: Update  $\mathbf{x}$  with incoming arrivals
6:   Let  $\Delta t$  be elapsed time since last update
7:   Update waiting cost:  $W \leftarrow W + \Delta t \cdot \sum_{i=1}^N c_i x_i$ 
8:   if  $\min_i x_i \geq 1$  then                                ▷ Feasible to match
9:     Compute current matching cost:  $M \leftarrow f(\mathbf{x})$ 
10:    if  $M \leq \alpha W$  then                                ▷ Cost balance condition
11:      Perform matching:  $\mathbf{x} \leftarrow \mathbf{x} - \mathbf{1}$           ▷ Match one tuple
12:      Update total cost:  $J \leftarrow J + W + M$ 
13:      Reset waiting cost:  $W \leftarrow 0$ 
14:    end if
15:  end if
16: end while
17: return  $J$ 
  
```

The intuition behind this design is as follows. Under Assumption 1, the matching cost $f(\mathbf{x})$ decreases as the queue lengths grow, reflecting the benefit of market thickness. Meanwhile, the waiting cost W accumulates over time as agents wait in the system. These two forces create opposing pressures: waiting longer reduces matching costs but increases waiting costs. The cost-balancing condition $M \leq \alpha W$ identifies the point at which further delay is no longer beneficial, as the marginal reduction in matching cost is outweighed by the accumulated waiting cost.

The CB algorithm offers three key advantages over existing approaches. First, it is adaptive: unlike fixed thresholds that must be recalibrated when demand patterns change, the CB algorithm automatically adjusts its matching frequency based on realized costs. In high-demand periods, waiting costs accumulate rapidly, triggering more frequent matches; in low-demand periods, the algorithm naturally waits longer to exploit market thickness. Second, it is computationally simple: implementation requires only tracking the queue lengths and a running sum of waiting costs, with no need for demand forecasting or complex optimization. Third, as we establish in the following subsection, the algorithm provides provable worst-case guarantees, ensuring robust performance even under adversarial arrival patterns.

3.3. Main Result

To evaluate the performance of online matching algorithms, we adopt the competitive ratio framework, which is the standard metric in online decision-making for comparing an algorithm's performance against an omniscient offline benchmark. Let J^{OPT} denote the minimum total cost achievable by an offline algorithm with complete knowledge of the arrival sequence in advance. The competitive ratio measures the worst-case performance gap between an online algorithm and this optimal benchmark.

DEFINITION 1 (COMPETITIVE RATIO). An online algorithm π is ρ -competitive if $\frac{J^\pi}{J^{OPT}} \leq \rho$ for all problem instances and arrival sequences. The competitive ratio of π is the infimum over all ρ for which this inequality holds.

A lower competitive ratio indicates better worst-case performance. An algorithm with competitive ratio ρ guarantees that its cost is at most ρ times the optimal offline cost, regardless of how adversarial the arrival pattern may be. This worst-case framework is particularly relevant for matching platforms, which face demand shocks, seasonal fluctuations, and non-stationary arrival patterns that are difficult to forecast. A bounded competitive ratio ensures that the algorithm performs well even in scenarios that were not anticipated during design.

Our main theoretical result establishes that the CB algorithm achieves a bounded competitive ratio.

THEOREM 1. *The Cost-Balancing algorithm with parameter $\alpha = \sqrt{\Gamma}$ is $(1 + \sqrt{\Gamma})$ -competitive, where*

$$\Gamma := \max_{\mathbf{x}, i} \frac{f(\mathbf{x})}{f(\mathbf{x} + \mathbf{e}_i)}$$

is the maximum ratio of matching costs before and after a single arrival.

The parameter $\Gamma \geq 1$ quantifies the economies of scale in the matching cost function. Specifically, Γ measures the maximum relative reduction in matching cost that can be achieved by adding one agent to the system. When Γ is close to 1, the matching cost is relatively insensitive to queue length, and the competitive ratio approaches 2. When Γ is larger, the matching cost drops more sharply with queue size, reflecting stronger economies of scale.

Theorem 1 has several important implications. First, the CB algorithm provides a guaranteed performance bound: its cost is at most $(1 + \sqrt{\Gamma})$ times the offline optimum, regardless of the arrival pattern. This guarantee holds even under adversarial arrivals where the arrival sequence is chosen to maximize the algorithm's cost. Second, the competitive ratio depends only on the structural parameter Γ , which is determined by the matching cost function, not by the arrival process. This means the same algorithm works well across different demand environments without re-tuning. Third, as we will demonstrate in Section 5, standard heuristics such as greedy matching and fixed-threshold policies can have unbounded competitive ratios, meaning their costs can be arbitrarily worse than the optimum in adversarial scenarios. The CB algorithm thus offers a qualitatively stronger guarantee than these common approaches.

The proof of Theorem 1 and additional theoretical results, including a lower bound on the competitive ratio achievable by any online algorithm, are presented in Section 5.

4. The Cost-Balancing Principle

The Cost-Balancing algorithm introduced in Section 3.2 is not an ad hoc heuristic; its design is grounded in the structural properties of optimal policies. This section develops the theoretical foundation underlying the cost-balancing principle. Our analysis proceeds in two stages. First, we examine a relaxed model with stationary arrivals to establish that optimal policies exhibit a monotone threshold structure, validating the search for threshold-type policies. Second, we employ fluid limit analysis to derive the precise relationship between waiting and matching costs at optimality. This analysis reveals that optimal performance is characterized by maintaining a specific ratio between accumulated waiting costs and instantaneous matching costs. The Cost-Balancing algorithm directly operationalizes this insight.

4.1. Monotonicity of Optimal Policies in Relaxed Settings

A fundamental question in matching algorithm design is whether simple threshold-type policies can be optimal. In general settings with arbitrary arrival patterns, the answer is often negative: the optimal decision rule can be highly complex and non-monotonic. However, when we restrict attention to stationary environments with well-behaved cost structures, a clear structure emerges.

We consider a relaxed model with Poisson arrivals and impose additional conditions on the matching cost function.

DEFINITION 2. A matching cost function $f : \mathbb{Z}_+^N \rightarrow \mathbb{R}_+$ is called convex, supermodular, and component-wise non-increasing if it satisfies the following properties:

- Convexity: $2f(\mathbf{x} + \mathbf{e}_i) \leq f(\mathbf{x}) + f(\mathbf{x} + 2\mathbf{e}_i)$ for all \mathbf{x} and i .
- Supermodularity: $f(\mathbf{x} + \mathbf{e}_i) + f(\mathbf{x} + \mathbf{e}_j) \leq f(\mathbf{x}) + f(\mathbf{x} + \mathbf{e}_i + \mathbf{e}_j)$ for all \mathbf{x} and $i \neq j$.
- Component-wise non-increasing: $f(\mathbf{x} + \mathbf{e}_i) \leq f(\mathbf{x})$ for all \mathbf{x} and i .

Convexity ensures diminishing marginal returns from additional agents, supermodularity captures complementarity across agent types, and the non-increasing property reflects economies of scale. Many natural matching cost functions satisfy these conditions. For example, in spatial matching where agents are uniformly distributed, the expected minimum distance decreases convexly in the number of agents.

Under these conditions, we establish the following structural result.

PROPOSITION 1. *Consider a matching system with Poisson arrivals and a matching cost function that is convex, supermodular, and component-wise non-increasing. The optimal policy is monotone in the queue length vector: if it is optimal to match at state \mathbf{x} , then it is also optimal to match at any state $\mathbf{y} \succeq \mathbf{x}$.*

REMARK 1. The proof of Proposition 1, detailed in Appendix EC.2.1, requires a novel analytical approach. Standard dynamic programming arguments establish monotonicity by propagating convexity or supermodularity of the value function across state transitions. However, these properties fail to hold in multi-sided matching due to the coupled state transitions: a single match simultaneously reduces all queue lengths by one ($\mathbf{x} \rightarrow \mathbf{x} - \mathbf{1}$), breaking the standard induction structure. We overcome this challenge by introducing a

diagonal difference function $G(\mathbf{x}) = J(\mathbf{x}) - J(\mathbf{x} - \mathbf{1})$ and establishing specialized bounds on its increments relative to the matching cost. This technique enables direct induction on the net matching benefit without requiring global structural properties of the value function.

Proposition 1 confirms that in stable environments, the intuition “more agents make matching more attractive” holds rigorously. The optimal policy takes a threshold form: match if and only if the queue lengths exceed certain thresholds.

However, this result also reveals a fundamental limitation: the optimal threshold depends on the arrival rate. A static threshold that is optimal for one arrival rate will be suboptimal when the rate changes. In practice, platforms face volatile demand patterns where arrival rates fluctuate significantly over time (e.g., peak vs. off-peak hours, weather events, special promotions). A fixed threshold policy, no matter how carefully calibrated, will perform poorly when conditions deviate from the assumed baseline. This observation motivates the search for an adaptive policy that adjusts its matching criterion in real-time without requiring knowledge of the arrival rate.

4.2. The Cost-Balancing Principle via Fluid Analysis

To understand how an optimal policy should adapt, we analyze a tractable special case using fluid limit techniques. The key insight from this analysis is that optimal behavior is characterized by a cost ratio condition, which forms the basis for the Cost-Balancing algorithm.

For tractability, we consider a symmetric two-sided system ($N = 2$) with Poisson arrivals at rate $\frac{\lambda}{2}$ for each type and equal waiting cost rates $c_1 = c_2 = c$. We focus on the two-sided case for clarity of exposition; we expect a similar cost-ratio characterization to hold for general N , though the optimal ratio may depend on the specific form of the cost function in the multi-sided case. We assume the matching cost follows a power-law form that explicitly captures economies of scale:

ASSUMPTION 2. *The matching cost function is $f(x_1, x_2) = \frac{\kappa}{(x_1 x_2)^\beta}$, where $\kappa > 0$ is a scale parameter and $\beta > 0$ controls the strength of economies of scale.*

This functional form satisfies Assumption 1: matching costs decrease as queue lengths grow. Such power-law cost structures arise naturally in spatial matching settings and have been widely adopted in the literature (e.g., [Wang et al. \(2024\)](#)). A larger β corresponds to stronger economies of scale, where the benefit of waiting (i.e., reduced matching cost) is more pronounced.

By analyzing the fluid limit of this system, where stochastic fluctuations average out, we can characterize the optimal policy explicitly.

THEOREM 2. *Consider the symmetric two-sided system under Assumption 2 with Poisson arrivals at rate $\lambda/2$ for each type and equal waiting cost rates $c_1 = c_2 = c$. In the fluid limit, the optimal policy maintains a constant ratio between the average waiting cost rate W^* and the average matching cost rate M^* :*

$$\frac{W^*}{M^*} = 2\beta,$$

where 2β is the elasticity of the matching cost function with respect to the common queue length.

Theorem 2 provides the key insight underlying the Cost-Balancing algorithm, it reveals that cost-balancing approximates optimal behavior in stable environments; the proof is postponed to Appendix EC.2.2. The ratio 2β , which measures the strength of economies of scale, determines the optimal balance point. When β is large (strong economies of scale), the optimal policy tolerates higher waiting costs relative to matching costs, because the benefit of accumulating more agents is substantial. When β is small (weak economies of scale), the optimal policy matches more promptly, as waiting provides limited benefit.

This result directly motivates the design of the CB algorithm. The algorithm triggers a match when the condition $M \leq \alpha W$ is satisfied. This condition forces the algorithm to maintain a cost ratio near $1/\alpha$, tracking the optimal fluid trajectory characterized by Theorem 2.

The cost-balancing principle also explains the algorithm's robustness to changing conditions. Consider what happens when the arrival rate suddenly increases. Higher arrival rates cause waiting costs to accumulate faster (more agents waiting per unit time), while matching costs decrease faster (queues grow more quickly). Both effects push the ratio W/M upward, causing the cost-balancing condition to be satisfied sooner. The algorithm thus automatically matches more frequently during high-demand periods. Conversely, when arrival rates decrease, waiting costs accumulate slowly, and the algorithm naturally waits longer to exploit market thickness. This automatic adaptation occurs without any knowledge of the arrival rate, because the algorithm responds directly to realized costs rather than forecasted demand.

Theorem 2 and Theorem 1 play distinct and complementary roles. Theorem 2 provides design motivation: it shows that in the fluid limit of a symmetric two-sided system with power-law costs, the optimal policy maintains a specific cost ratio $W^*/M^* = 2\beta$, revealing the cost-balancing principle as the structural driver of optimal behavior. Theorem 1 provides a performance guarantee: using $\alpha = \sqrt{\Gamma}$, the CB algorithm achieves a competitive ratio of $(1 + \sqrt{\Gamma})$ under adversarial arrivals for general cost functions satisfying Assumption 1. The key point is that the fluid analysis identifies what principle to use (balance costs), while the competitive analysis determines how to calibrate it for worst-case robustness.

5. Competitive Ratio Analysis

This section provides rigorous performance guarantees for the Cost-Balancing algorithm and establishes fundamental limits on what any online algorithm can achieve. Our analysis yields three main results. First, we prove that the CB algorithm achieves a competitive ratio of $(1 + \sqrt{\Gamma})$, guaranteeing that its cost is within a constant factor of the offline optimum regardless of the arrival pattern (Section 5.1). Second, we demonstrate that standard heuristics, including greedy and fixed-threshold policies, have unbounded competitive ratios, meaning they can perform arbitrarily worse than the optimum in adversarial scenarios (Section 5.2). Third, we establish a universal lower bound of $(\sqrt{5} + 1)/2$ (the golden ratio) on the competitive ratio achievable by any online algorithm, quantifying the fundamental price of uncertainty in this problem (Section 5.3). All analysis is conducted on the base model defined in Section 3.

5.1. Proof of the Main Theorem

We now prove Theorem 1, which states that the CB algorithm with parameter $\alpha = \sqrt{\Gamma}$ achieves a competitive ratio of $(1 + \sqrt{\Gamma})$. The proof employs a charging argument: we show that by maintaining a balance between waiting and matching costs, the CB algorithm ensures that any cost it incurs can be charged to a corresponding cost incurred by the optimal offline algorithm, with a bounded inflation factor.

Proof of Theorem 1. Consider the CB algorithm with parameter $\alpha = \sqrt{\Gamma}$. Let τ_k be the time of the k -th match under the CB algorithm, and let \mathbf{x}_k and W_k be the system state and accumulated waiting cost at time τ_k , respectively. Similarly, let \mathbf{x}_k^- and W_k^- denote the state and accumulated waiting cost just prior to the arrival that triggered the k -th match.

By the design of Algorithm 1, a match is triggered only when the matching cost $f(\mathbf{x})$ is no more than α times the accumulated waiting cost W . Therefore, at the moment of the k -th match, we have the inequality $f(\mathbf{x}_k) \leq \alpha W_k$, which implies $\frac{f(\mathbf{x}_k)}{W_k} \leq \alpha$.

On the other hand, just before the triggering arrival (at state \mathbf{x}_k^-), the condition for matching was not met (otherwise a match would have occurred earlier). Thus, we have $f(\mathbf{x}_k^-) > \alpha W_k^-$. Since the waiting cost function $W(t)$ is continuous and non-decreasing, and the transition from state \mathbf{x}_k^- to \mathbf{x}_k is instantaneous (a single arrival), we have $W_k^- = W_k$. Using the definition of Γ , we know that the matching cost can decrease by at most a factor of Γ upon a single arrival, i.e., $f(\mathbf{x}_k^-) \leq \Gamma f(\mathbf{x}_k)$. Combining these gives $\alpha W_k = \alpha W_k^- < f(\mathbf{x}_k^-) \leq \Gamma f(\mathbf{x}_k)$, which implies $\frac{f(\mathbf{x}_k)}{W_k} > \frac{\alpha}{\Gamma}$.

Setting $\alpha = \sqrt{\Gamma}$, we obtain the following bounds relating the matching and waiting costs at decision epochs:

$$\frac{1}{\sqrt{\Gamma}} < \frac{f(\mathbf{x}_k)}{W_k} \leq \sqrt{\Gamma}. \quad (1)$$

This relationship (1) is key to establishing the competitive ratio.

We now proceed to prove the theorem by showing that the total cost incurred by any two consecutive matches under the OPT is at least $\frac{1}{1+\sqrt{\Gamma}}$ of the corresponding cost under the CB algorithm. Consider the interval between the k -th and $(k+1)$ -th matches of the CB algorithm and the optimal algorithm. For a given k , we seek to lower bound the cost of OPT, specifically $(f(\mathbf{x}_k^{OPT}) + W_k^{OPT}) + (f(\mathbf{x}_{k+1}^{OPT}) + W_{k+1}^{OPT})$, relative to CB's cost.

We divide the analysis into cases based on the timing of OPT's matches relative to CB's matches (τ_k denotes the time of the k -th match for CB, and τ_k^{OPT} for OPT).

- Case 1: $\tau_k^{OPT} \leq \tau_k$, then due to Assumption 1 (monotonicity), we have $f(\mathbf{x}_k^{OPT}) \geq f(\mathbf{x}_k)$. If $\tau_{k+1}^{OPT} > \tau_{k+1}$, then the interval $[\tau_k^{OPT}, \tau_{k+1}^{OPT}]$ covers the interval $[\tau_k, \tau_{k+1}]$. Consequently, OPT accumulates waiting cost during this entire period. Thus, $W_{k+1}^{OPT} \geq W_{k+1}$ (since CB clears at τ_{k+1} but OPT waits longer). Then we have:

$$(f(\mathbf{x}_k^{OPT}) + W_k^{OPT}) + (f(\mathbf{x}_{k+1}^{OPT}) + W_{k+1}^{OPT})$$

$$\geq f(\mathbf{x}_k) + W_{k+1} \geq \frac{1}{1 + \sqrt{\Gamma}} [(f(\mathbf{x}_k) + W_k) + (f(\mathbf{x}_{k+1}) + W_{k+1})],$$

where the last inequality follows from (1).

If $\tau_{k+1}^{OPT} \leq \tau_{k+1}$, then OPT matches with fewer agents at $(k+1)$'s match, its matching cost is higher. Specifically, $f(\mathbf{x}_{k+1}^{OPT}) \geq f(\mathbf{x}_{k+1})$. Then we have:

$$\begin{aligned} & (f(\mathbf{x}_k^{OPT}) + W_k^{OPT}) + (f(\mathbf{x}_{k+1}^{OPT}) + W_{k+1}^{OPT}) \\ & \geq f(\mathbf{x}_k) + f(\mathbf{x}_{k+1}) \geq \frac{1}{1 + \sqrt{\Gamma}} [(f(\mathbf{x}_k) + W_k) + (f(\mathbf{x}_{k+1}) + W_{k+1})]. \end{aligned}$$

- Case 2: $\tau_k^{OPT} > \tau_k$. If $\tau_{k+1}^{OPT} > \tau_{k+1}$, then we have $W_k^{OPT} + W_{k+1}^{OPT} \geq W_k + W_{k+1}$. It follows from (1) that

$$\begin{aligned} & (f(\mathbf{x}_k^{OPT}) + W_k^{OPT}) + (f(\mathbf{x}_{k+1}^{OPT}) + W_{k+1}^{OPT}) \\ & \geq W_k + W_{k+1} \geq \frac{1}{1 + \sqrt{\Gamma}} [(f(\mathbf{x}_k) + W_k) + (f(\mathbf{x}_{k+1}) + W_{k+1})]. \end{aligned}$$

If $\tau_{k+1}^{OPT} \leq \tau_{k+1}$, then similar to Case 1, we have $f(\mathbf{x}_{k+1}^{OPT}) \geq f(\mathbf{x}_{k+1})$, thus we have:

$$\begin{aligned} & (f(\mathbf{x}_k^{OPT}) + W_k^{OPT}) + (f(\mathbf{x}_{k+1}^{OPT}) + W_{k+1}^{OPT}) \\ & \geq W_k + f(\mathbf{x}_{k+1}) \geq \frac{1}{1 + \sqrt{\Gamma}} [(f(\mathbf{x}_k) + W_k) + (f(\mathbf{x}_{k+1}) + W_{k+1})]. \end{aligned}$$

In all cases, the cost of OPT is lower bounded by $\frac{1}{1 + \sqrt{\Gamma}}$ of the cost of CB. Summing over all k , we obtain the competitive ratio. \square

REMARK 2. The proof pairs two consecutive matches of CB and OPT rather than comparing them one-to-one. A one-to-one comparison fails because CB and OPT may match at different times: a single OPT match may occur between two CB matches (or vice versa), so there is no natural one-to-one correspondence. By grouping consecutive CB matches into pairs, the case analysis covers all possible timings of OPT matches relative to each pair, yielding a complete partition of the cost accounting.

5.2. The Fragility of Standard Heuristics

To appreciate the value of this guarantee, it is instructive to compare it with the performance of standard policies widely used in practice. We show that while heuristics like Greedy and Fixed Thresholds may perform well in stable, average-case scenarios, they are fundamentally brittle: they lack the “safety net” mechanism of Cost-Balancing and can incur unbounded relative costs in adversarial environments.

The Greedy policy matches immediately whenever feasible ($\min_i X_i \geq 1$), prioritizing minimal waiting at the expense of matching quality. While greedy policies can achieve near-optimal performance under specific conditions such as certain graph structures (Gupta 2024), they generally underperform when matching costs exhibit significant economies of scale.

PROPOSITION 2. *The competitive ratio of the Greedy policy is unbounded.*

Proof of Proposition 2. We construct an adversarial arrival sequence that drives the competitive ratio to infinity. Consider n complete tuples (one agent of each type) arriving at times $t_k = k\epsilon$ for $k = 0, 1, \dots, n-1$, where $\epsilon > 0$ is arbitrarily small. Assume the matching cost function satisfies $f(k \cdot \mathbf{1}) = c/k$ for some constant $c > 0$, which satisfies Assumption 1 (non-increasing in queue lengths).

Under the Greedy policy, at each arrival time t_k , exactly one agent of each type is present in the queue, since the previous tuple was matched immediately upon its arrival. Therefore, Greedy executes each match at state $\mathbf{1}$, incurring cost $f(\mathbf{1}) = c$ per match. The total cost under Greedy is $J^{Greedy} = n \cdot c + W^{Greedy}$, where $W^{Greedy} \leq n \cdot (\sum_i c_i) \cdot \epsilon \rightarrow 0$ as $\epsilon \rightarrow 0$.

In contrast, the optimal policy waits until time $t_{n-1} = (n-1)\epsilon$ when all n tuples have arrived, then executes n consecutive matches. The j -th match ($j = 1, \dots, n$) occurs at state $(n-j+1) \cdot \mathbf{1}$, incurring cost $f((n-j+1) \cdot \mathbf{1}) = c/(n-j+1)$. The total matching cost is $\sum_{k=1}^n c/k = c \cdot H_n$, where $H_n = \sum_{k=1}^n 1/k$ is the n -th harmonic number. The waiting cost satisfies $W^{OPT} \leq n \cdot (\sum_i c_i) \cdot (n-1)\epsilon \rightarrow 0$ as $\epsilon \rightarrow 0$.

Comparing these costs, as $\epsilon \rightarrow 0$, the competitive ratio satisfies

$$\frac{J^{Greedy}}{J^{OPT}} \rightarrow \frac{n \cdot c}{c \cdot H_n} = \frac{n}{H_n}.$$

Since $H_n \sim \ln n$ as $n \rightarrow \infty$, we have $n/H_n \rightarrow \infty$. Therefore, the competitive ratio of the Greedy policy is unbounded. \square

The Threshold policy waits until the queue length reaches a fixed threshold θ before matching, deliberately accumulating agents to exploit economies of scale. This approach is prevalent in periodic clearing models (Kerimov et al. 2024) and can achieve asymptotically optimal performance in thick markets (Eom and Toriello 2025). However, the optimal threshold depends on arrival rates, making fixed thresholds fragile to demand fluctuations.

PROPOSITION 3. *The competitive ratio of the Threshold policy is unbounded.*

Proof of Proposition 3. We construct an adversarial arrival sequence that drives the competitive ratio to infinity. Consider a threshold policy with parameter $\theta \geq 2$, which triggers a match only when $\min_i X_i \geq \theta$.

At time $t = 0$, suppose $\theta - 1$ agents of each type arrive simultaneously, so the system state is $(\theta - 1) \cdot \mathbf{1}$. Since $\min_i X_i = \theta - 1 < \theta$, the threshold policy does not match and waits for additional arrivals. Let the next arrival occur at time $t = T$ for some $T > 0$.

Under the Threshold policy, all $(\theta - 1) \cdot N$ agents wait in the system for the entire interval $[0, T]$. The waiting cost incurred is $W^{Threshold} = (\theta - 1) \cdot (\sum_{i=1}^N c_i) \cdot T$. After the arrival at time T , the policy executes matches, incurring additional matching costs. Thus, the total cost satisfies $J^{Threshold} \geq (\theta - 1) \cdot (\sum_{i=1}^N c_i) \cdot T$.

In contrast, the optimal policy matches all $\theta - 1$ tuples immediately at time $t = 0$. The total cost is $J^{OPT} = \sum_{k=1}^{\theta-1} f(k \cdot \mathbf{1})$, which is bounded and independent of T .

The competitive ratio satisfies

$$\frac{J^{Threshold}}{J^{OPT}} \geq \frac{(\theta - 1) \cdot (\sum_{i=1}^N c_i) \cdot T}{\sum_{k=1}^{\theta-1} f(k \cdot \mathbf{1})} \rightarrow \infty \quad \text{as } T \rightarrow \infty.$$

Therefore, the competitive ratio of the Threshold policy is unbounded. \square

The unbounded competitive ratios of Greedy and Threshold policies stem from a common structural flaw: both commit to a fixed decision rule that ignores the realized state of the system. Greedy always matches immediately, regardless of how much matching cost could be saved by waiting; Threshold always waits to θ , regardless of how much waiting cost has accumulated. In adversarial scenarios, these rigid commitments can be exploited: an adversary can construct arrival sequences that maximize the gap between the policy's cost and the optimal cost.

The CB algorithm avoids this vulnerability by conditioning its decision on the ratio of realized costs. The cost-balancing condition $M \leq \alpha W$ creates a decision boundary that shifts with the state of the system: the more waiting cost has accumulated, the higher matching cost the algorithm is willing to accept. This state-dependent threshold ensures that no single adversarial arrival pattern can drive the cost ratio to infinity, which is the key mechanism underlying the bounded competitive ratio guarantee.

5.3. The Price of Uncertainty

Having shown that the CB algorithm achieves a bounded competitive ratio while standard heuristics do not, a natural question arises: how close to optimal can any online algorithm be? We establish a fundamental lower bound showing that no online algorithm can achieve a competitive ratio better than the golden ratio $(\sqrt{5} + 1)/2 \approx 1.618$. The construction follows the classical “rent-or-buy” structure from online algorithms: the adversary forces any algorithm into a dilemma between acting too early (missing economies of scale) and acting too late (accumulating excessive waiting costs).

PROPOSITION 4. *The competitive ratio of any online algorithm is at least $(\sqrt{5} + 1)/2$.*

Proof of Proposition 4. We prove the lower bound by constructing an adversarial instance that forces any online algorithm into a dilemma between matching too early (missing economies of scale) and matching too late (incurring excessive waiting costs). Following the approach of Bhimaraju et al. (2026), consider a single-type matching system where each match pairs two agents.

At time $t = 0$, suppose $2n$ agents arrive. Let ALG be any deterministic online algorithm, and suppose ALG makes its first match at time $t = \Delta t \geq 0$. The adversary observes Δt and chooses between two scenarios.

In Scenario 1, no further arrivals occur after $t = 0$. ALG incurs waiting cost $2n\Delta t$ (with unit waiting cost rate) before executing n matches at pool sizes $2n, 2n - 2, \dots, 2$, yielding matching cost $\sum_{i=1}^n f(2i)$. The optimal offline policy matches immediately at $t = 0$, incurring only matching cost $\sum_{i=1}^n f(2i)$. Thus, the competitive ratio satisfies

$$\rho \geq \frac{2n\Delta t + \sum_{i=1}^n f(2i)}{\sum_{i=1}^n f(2i)}. \quad (2)$$

In Scenario 2, an additional $2n$ agents arrive at time $t = \Delta t + \epsilon$ for arbitrarily small $\epsilon > 0$. Due to its online nature, ALG cannot anticipate these arrivals and has already committed to matching at time Δt . Consequently, ALG matches once before the second batch arrives, then continues matching the remaining agents from both batches. Since ALG processes the two batches partially separately, its total cost is at least $2n\Delta t + 2 \sum_{i=1}^n f(2i)$. In contrast, the optimal offline policy waits until $t = \Delta t + \epsilon$ when all $4n$ agents are present, then matches from the combined pool. The optimal cost is $2n(\Delta t + \epsilon) + \sum_{i=1}^{2n} f(2i)$. Thus, the competitive ratio satisfies

$$\rho \geq \frac{2n\Delta t + 2 \sum_{i=1}^n f(2i)}{2n(\Delta t + \epsilon) + \sum_{i=1}^{2n} f(2i)}. \quad (3)$$

Since the adversary chooses the scenario that maximizes the ratio, we have $\rho \geq \max\{(2), (3)\}$. Taking $\epsilon \rightarrow 0$ and letting $S = \sum_{i=1}^n f(2i)$ and $S' = \sum_{i=1}^{2n} f(2i)$, we obtain

$$\rho \geq \max \left\{ 1 + \frac{2n\Delta t}{S}, \frac{2n\Delta t + 2S}{2n\Delta t + S'} \right\}.$$

The algorithm's best choice of Δt minimizes this maximum, which occurs when the two terms are equal. Setting them equal and solving yields $\rho \geq 1 + \frac{1}{2} \left(-a + \sqrt{a^2 - 4a + 8} \right)$, where $a = S'/S \in [1, 2]$.

Since this lower bound is decreasing in a , the tightest bound is achieved as $a \rightarrow 1$, which occurs when n is large enough and $f(n+i) \ll f(i)$. Substituting $a = 1$ gives $\rho \geq 1 + \frac{1}{2} \left(-1 + \sqrt{5} \right) = \frac{\sqrt{5}+1}{2}$.

Therefore, no online algorithm can achieve a competitive ratio better than the golden ratio $(\sqrt{5} + 1)/2$.

□

Proposition 4 quantifies the fundamental price of uncertainty in online matching. Even an algorithm with unlimited computational power cannot achieve a competitive ratio below $(\sqrt{5} + 1)/2$ without knowledge of future arrivals. This lower bound is tight in the sense that it is achieved by a specific problem instance; it represents an inherent limitation of online decision-making rather than algorithmic inefficiency.

6. Discussion on Model with Attribute Information

Our main analysis rests on Assumption 1, which posits that matching costs depend on queue lengths (market thickness) rather than the microscopic attributes of individual agents. While real-world costs are indeed attribute-dependent, it is natural to ask what happens when full attribute information is incorporated into the online decision-making framework. In this section, we first formally define the general attribute-based model, then characterize two fundamental barriers that arise: computational intractability and theoretical impossibility of bounded competitive ratios under adversarial arrivals.

6.1. The General Attribute-Based Model

We now formally define the general matching model with attribute information, which extends the queue-based model in Section 3.1.

In the attribute-based model, each arriving agent carries relevant attributes drawn from an attribute space Q . Specifically, the n -th type- i agent arrives with attribute $q_{in} \in Q$ drawn from a type-specific distribution ν_i . These attributes encode agent-specific information relevant to matching quality: geographic locations in ride-sharing, skill ratings in gaming, or delivery destinations in logistics.

The system state at time t consists of two components:

1. The queue length vector $\mathbf{X}(t) = (X_1(t), \dots, X_N(t)) \in \mathbb{Z}_+^N$, where $X_i(t)$ is the number of unmatched type- i agents.
2. The attribute configuration $\mathbf{Q}(t) = \{q_{ij} : j \leq X_i(t), i \in \{1, \dots, N\}\}$, collecting the attributes of all unmatched agents.

In this general model, the matching cost depends on the specific agents selected for a match. Let $f(q_1, \dots, q_N)$ denote the cost of matching a tuple of agents with attributes (q_1, \dots, q_N) . When the controller decides to match at state (\mathbf{X}, \mathbf{Q}) , it selects one agent from each type to minimize the matching cost:

$$f^*(\mathbf{X}, \mathbf{Q}) := \min_{j_i \leq X_i, \forall i} f(q_{1,j_1}, \dots, q_{N,j_N}).$$

A policy π in this model is a mapping from the full state $(\mathbf{X}, \mathbf{Q}, t)$ to a matching decision. The monotonicity property of the matching cost function is modified accordingly for the general attribute-based model.

ASSUMPTION 3. *The matching cost incurred at time t is a function $f^*(\cdot, \cdot)$, which depends on $\{X_i(t), 1 \leq i \leq N\}$, the number of unmatched agents at time t for each type, and the attributes $\{Q_i(t), 1 \leq i \leq N\}$ of all unmatched agents. Furthermore, $f^*(\cdot, \cdot)$ satisfies the monotonicity property, i.e., $f^*(\mathbf{x}, \mathbf{q}_x) \leq f^*(\mathbf{y}, \mathbf{q}_y)$ whenever $\mathbf{x} \succeq \mathbf{y}$ and the attributes \mathbf{q}_y are a subcollection of \mathbf{q}_x (i.e., the set of agents in the queues for \mathbf{y} is a subset of those for \mathbf{x}).*

The queue-based model in our main analysis (Assumption 1) can be viewed as a tractable approximation where the matching cost $f(\mathbf{X})$ depends only on queue lengths, not on specific attribute realizations. This approximation is justified when larger pools statistically yield better matches, which holds in most practical settings. The following results characterize the computational and information-theoretic barriers inherent to this general formulation.

6.2. Computational Intractability

We first address computational feasibility. Even in a static setting where all agents are present simultaneously, finding the cost-minimizing match is prohibitively difficult for multi-sided markets.

PROPOSITION 5. *For $N \geq 3$, computing an optimal matching in the attribute-based model is NP-hard, even in a static one-shot setting with zero waiting costs.*

Proof. Consider a static instance where all agents arrive at $t = 0$, waiting costs are zero ($c_i = 0$ for all i), and the controller must partition agents into disjoint N -tuples to minimize total matching cost. For $N = 3$, this reduces to the 3-Dimensional Matching (3DM) problem.

Let there be n agents of each type with attribute sets $Q_1 = \{q_{1,1}, \dots, q_{1,n}\}$, $Q_2 = \{q_{2,1}, \dots, q_{2,n}\}$, $Q_3 = \{q_{3,1}, \dots, q_{3,n}\}$. Let $T \subseteq Q_1 \times Q_2 \times Q_3$ be a set of feasible triples. Define the matching cost as

$$f(q_{1,i}, q_{2,j}, q_{3,k}) = \begin{cases} 0 & \text{if } (q_{1,i}, q_{2,j}, q_{3,k}) \in T, \\ 1 & \text{otherwise.} \end{cases}$$

Finding a matching with total cost zero is equivalent to finding a perfect 3-dimensional matching, which is NP-complete (Karp 1972). Since the dynamic problem generalizes this static instance, computing optimal policies in the attribute-based model is NP-hard. \square

The hardness result extends to any $N \geq 3$ via reduction to N -dimensional matching. For $N = 2$, the static assignment is polynomial-time solvable as minimum-weight bipartite matching (Kuhn 1955), but the dynamic problem remains intractable due to the continuous attribute state space and infinite horizon.

This result has important practical implications. For platforms coordinating three or more agent types (e.g., rider, driver, and restaurant in food delivery), even computing the optimal match for a fixed set of agents is computationally prohibitive. Dynamic optimization over an infinite horizon is even more demanding. By abstracting attributes into aggregate queue lengths, we bypass this combinatorial explosion, focusing on the temporal trade-offs that are central to dynamic matching control.

6.3. Theoretical Impossibility Under Adversarial Attributes

Beyond computational hardness, there is a more fundamental barrier: the impossibility of bounded competitive ratios when the adversary controls agent attributes. In our main model, adversarial arrivals are restricted to timing; attributes are abstracted into queue lengths. Here we show that if the adversary can also choose specific agent attributes, no online algorithm can achieve bounded performance guarantees.

PROPOSITION 6. *In the attribute-based model where the adversary controls both arrival times and agent attributes, no online algorithm achieves a bounded competitive ratio.*

Proof of Proposition 6. We construct an adversarial strategy that forces any online algorithm to have unbounded competitive ratio by exploiting attribute-dependent costs. Consider a two-sided matching problem ($N = 2$) in the general attribute-based model of Section 6.1, where the matching cost for a pair of attributes $(q_1, q_2) \in Q \times Q$ is given by a function $f(q_1, q_2)$, and the waiting cost rate is $c > 0$ per agent per unit time.

Fix four attributes $a_1, a_2, b_1, b_2 \in Q$ such that

$$f(a_1, b_1) = M_1,$$

$$f(a_1, b_2) = 0,$$

$$f(a_2, b_1) = 0,$$

$$f(a_2, b_2) = M_2,$$

where $M_1 > 0$ and $M_2 \gg M_1$ will be chosen by the adversary. It is straightforward to verify that this definition of $f(\cdot, \cdot)$ satisfies Assumption 3.

At time $t = 0$, a type-1 agent with attribute a_1 and a type-2 agent with attribute b_1 arrive. Let ALG be any deterministic online algorithm, and let $\tau \geq 0$ be the time at which ALG decides to match this pair (if ALG never matches them, we may treat τ as arbitrarily large and the argument below becomes even stronger). At time $\tau + \epsilon$ (for arbitrarily small $\epsilon > 0$), the adversary adapts based on ALG's choice of τ and decides whether to send an additional pair of agents.

Case 1 (adversary sends new agents): At time $\tau + \epsilon$, the adversary sends a type-1 agent with attribute a_2 and a type-2 agent with attribute b_2 . ALG has already matched the initial pair at time τ , incurring matching cost M_1 and waiting cost $2c\tau$, for a total of $M_1 + 2c\tau$. When the new pair (a_2, b_2) arrives, ALG must eventually match them as well, incurring an additional cost of at least M_2 . Thus,

$$J^{ALG} \geq M_1 + M_2 + 2c\tau.$$

In contrast, the optimal offline policy waits until time $\tau + \epsilon$, when all four agents are present, and matches (a_1, b_2) and (a_2, b_1) , both at zero cost. The offline policy pays only waiting costs:

$$J^{OPT} = 2c(\tau + \epsilon) + 2c\epsilon \rightarrow 2c\tau \quad \text{as } \epsilon \rightarrow 0.$$

Hence, in this case the competitive ratio satisfies

$$\rho_1(\tau) \geq \frac{M_1 + M_2 + 2c\tau}{2c\tau} = 1 + \frac{M_1 + M_2}{2c\tau}.$$

Case 2 (adversary sends no further agents): No additional agents arrive after $t = 0$. ALG matches the initial pair at time τ , incurring total cost

$$J^{ALG} = M_1 + 2c\tau.$$

The optimal offline policy matches them immediately at $t = 0$, incurring cost

$$J^{OPT} = M_1.$$

The competitive ratio in this case is

$$\rho_2(\tau) = \frac{M_1 + 2c\tau}{M_1} = 1 + \frac{2c\tau}{M_1}.$$

The adversary, observing the algorithm's choice of τ , selects the worse of the two cases, so any deterministic ALG faces a competitive ratio at least

$$\rho(\tau) \geq \max\{\rho_1(\tau), \rho_2(\tau)\} = \max\left\{1 + \frac{M_1 + M_2}{2c\tau}, 1 + \frac{2c\tau}{M_1}\right\}.$$

To minimize this worst-case ratio, ALG would choose τ to minimize the right-hand side. Let $u = \frac{c\tau}{M_1} > 0$. Then

$$\rho(u) \geq \max \left\{ 1 + \frac{1 + M_2/M_1}{2u}, 1 + 2u \right\}.$$

The minimum of this maximum occurs when the two terms are equal:

$$1 + \frac{1 + M_2/M_1}{2u} = 1 + 2u \implies \frac{1 + M_2/M_1}{2u} = 2u \implies u^2 = \frac{1 + M_2/M_1}{4}.$$

Substituting this value of u into the ratio gives

$$\rho \geq 1 + 2u = 1 + \sqrt{1 + M_2/M_1}.$$

Then the adversary can choose attributes and cost parameters so that the ratio M_2/M_1 is arbitrarily large. As $M_2/M_1 \rightarrow \infty$, we have $\rho \rightarrow \infty$. Thus, for any proposed competitive ratio bound $R < \infty$, the adversary can pick attributes with M_2/M_1 large enough so that

$$1 + \sqrt{1 + M_2/M_1} > R.$$

Therefore, no online algorithm achieves a bounded competitive ratio when the adversary can control both arrival times and attributes. \square

This impossibility result reveals a fundamental tension: no online algorithm can simultaneously be robust to adversarial attributes and adversarial arrival timing. The adversary can always exploit the algorithm's ignorance of future attribute realizations to create arbitrarily bad outcomes.

These results clarify the role of the queue-based abstraction (Assumption 1). By modeling matching costs as functions of queue lengths rather than individual attributes, the queue-based model captures the empirical regularity that larger pools yield better matches on average, without requiring the algorithm to predict specific attribute realizations. This abstraction enables the bounded competitive ratio guarantee of Theorem 1 by restricting the adversary's power to arrival timing, which is the primary source of uncertainty in platform operations.

7. Numerical Study

This section validates the practical effectiveness of the Cost-Balancing algorithm through experiments on two real-world applications: video game matchmaking and on-demand food delivery. These settings test the algorithm beyond the stylized assumptions of our theoretical model. In particular, while our theory assumes queue-dependent matching costs (Assumption 1), the experiments use full attribute-based costs (skill ratings in gaming, geographic locations in delivery). The theoretical competitive ratio guarantee (Theorem 1) does not directly apply to these settings. Rather, the experiments test whether the cost-balancing principle, the idea of triggering matches based on the ratio of realized costs, generalizes beyond the model for which it was formally derived.

7.1. Video Game Matchmaking

We first examine a 1-vs-1 competitive gaming matchmaking system, where the platform must balance two objectives: minimizing player waiting time and ensuring skill-balanced matches. This setting introduces complexities absent from our theoretical model: agent heterogeneity is continuous (Elo skill ratings) rather than categorical.

We adopt the simulation environment of [Gan \(2023\)](#), which models player arrivals as a non-stationary Poisson process with hourly rates ranging from 0.32 to 0.60 to simulate daily traffic cycles. Each arriving player has a skill rating (Elo score) drawn from $\mathcal{N}(650, 225^2)$, truncated below at zero. The platform's objective is to minimize total cost, defined as

$$J = \sum_{k=1}^n w_k + \gamma \sum_{(i,j) \in \mathcal{M}} |s_i - s_j|,$$

where w_k denotes the waiting time of player k , $|s_i - s_j|$ is the skill gap for matched pair (i, j) , and $\gamma > 0$ is a weight parameter governing the trade-off between responsiveness and match quality. The matching cost here is attribute-dependent (skill gap), testing the CB algorithm when [Assumption 1](#) is only an approximation.

We compare the CB algorithm against two benchmarks:

- Bubble Algorithm ([Gan 2023](#)): The industry-standard heuristic in gaming. Each player's search radius expands linearly over time; a match occurs when two radii overlap. This policy implicitly trades off skill gap against waiting time at the individual level.
- Threshold Policy: Matches the closest skill pairs whenever the queue size reaches a fixed threshold, exploiting market thickness to improve match quality.

For the CB algorithm, we track the total accumulated waiting time of all queued players as the waiting cost, and use the minimum achievable skill gap as the matching cost. A match is triggered when the matching cost falls below a scaled multiple of the accumulated waiting cost.

We simulate 100 player arrivals per episode, averaged over 100 independent runs. All algorithm parameters (expansion rate for Bubble, queue threshold for Threshold, scaling factor α for CB) are optimized via grid search for each value of γ .

[Table 1](#) reports the total system costs. The CB algorithm achieves the lowest cost across all values of γ , outperforming both the industry-standard Bubble algorithm and the Threshold policy. The improvement over Bubble ranges from 1.64% to 6.16%, with larger gains at extreme values of γ (either very low or very high).

These results illustrate two key advantages of the cost-balancing approach. First, unlike Bubble which makes local decisions based on individual player waiting times, CB aggregates system-wide waiting costs, enabling globally optimal timing decisions. During congestion, accumulated waiting costs grow rapidly, triggering faster matches to clear backlogs; during lulls, the algorithm naturally waits longer to improve

match quality. Second, unlike the Threshold policy which commits to a fixed queue size, CB adapts its effective threshold based on the realized cost ratio, responding flexibly to non-stationary demand patterns. This confirms that the cost-balancing principle generalizes effectively to continuous-attribute settings with non-stationary dynamics.

γ	Bubble	CB	Threshold	Improvement over Bubble (%)
1	10153.01	9527.43	10512.58	6.16
2	14336.47	13821.52	14378.55	3.59
3	17583.85	17150.54	18316.29	2.46
4	20399.40	19856.87	20800.71	2.66
5	22686.09	22313.19	22921.68	1.64
6	25148.93	24521.48	25151.21	2.49
7	27565.19	26514.22	27735.21	3.81
8	29958.64	28400.72	29393.03	5.20
9	31805.22	30149.87	30600.90	5.20
10	32914.03	31971.16	32305.72	2.86

Table 1 Comparison of the CB algorithm and two benchmark policies.

7.2. On-Demand Last-Mile Delivery

We now examine an on-demand last-mile delivery problem using real-world data from a food delivery platform in Shanghai, China. The data set, adapted from Liu et al. (2021), contains order and delivery records over a two-month period in 2015. In this setting, drivers collect meal boxes from a central depot, deliver all assigned orders, and return to the depot before receiving new assignments. Once dispatched, drivers cannot be rerouted to additional orders. The service provider faces a fundamental trade-off: waiting longer allows more orders and drivers to accumulate, enabling better matching and routing efficiency, but increases customer waiting time and risks violating delivery commitments.

7.2.1. Problem Setting

The delivery operation involves three sequential decisions:

1. Dispatch timing: Upon receiving new orders from customer locations \mathcal{I} at time t , the service provider decides whether to dispatch the current pool of orders and drivers or to wait. If the decision is to wait, the system holds for a unit time interval Δt and reevaluates.
2. Order assignment: When a dispatch is triggered, the provider assigns a subset of locations \mathcal{I}_k to each driver k from the available driver pool \mathcal{K} . Each driver has a capacity constraint limiting the number of orders they can carry.
3. Route planning: Each driver k plans a delivery route that starts and ends at the central depot, visiting all assigned locations \mathcal{I}_k . The route determines the total travel time $l_k(\mathcal{I}_k)$.

The service provider's objective is to minimize the total delivery delay across all dispatches. Let \tilde{t}_i denote the service time at customer location i (time spent at the location for handoff), and let $l_k(\mathcal{I}_k)$ denote the total

travel time of driver k given the assigned locations. The delivery delay for driver k is the amount by which the total delivery time exceeds the commitment time T_c . Summing over all drivers, the total delay is:

$$H = \sum_{k \in \mathcal{K}} \left(\sum_{i \in \mathcal{I}_k} \tilde{t}_i + l_k(\mathcal{I}_k) - T_c \right)^+, \quad (4)$$

where $(x)^+ = \max(x, 0)$ captures that only positive delays count. The commitment time T_c is adjusted as $T_c = T_0 - (\text{waiting time})$, where T_0 is the initial commitment and the waiting time accounts for how long orders have been held before dispatch. This adjustment ensures that customers who wait longer before dispatch receive correspondingly tighter delivery windows.

The order assignment problem (Stage 2) is formulated as a vehicle routing problem (VRP) with capacity constraints, where the objective is to minimize total delay subject to each driver's capacity limit. The VRP formulation, constraint descriptions, and solution methodology are provided in Appendix EC.1.1.

This delivery setting deviates from the base model in Section 3 in an important way. The base model considers symmetric multi-sided matching where each match forms a complete tuple with one agent from each type (e.g., one rider matched with one driver). In contrast, the delivery problem involves asymmetric one-to-many matching: each driver can be assigned multiple orders, and the matching cost depends on the entire assignment rather than individual pairings. This extension tests whether the cost-balancing principle, which was derived from the symmetric setting, can generalize to more complex matching structures encountered in practice.

7.2.2. Experimental Setup The data set contains 17,645 customer orders and 3,411 driver arrivals across 839 customer locations. We focus on lunch peak periods with batches containing more than 20 orders, yielding 179 batches with an average of 86 orders per batch, where each batch is 15 minutes long. For each batch, we randomly sample order and driver arrival times within the batch window to simulate arrival variability, repeating this five times to obtain 895 batch samples. The data is split into 716 training batches and 179 test batches. Key parameters are set as follows: initial commitment time $T_0 = 35$ minutes, driver capacity $C = 30$ meal boxes, and decision granularity $\Delta t = 1$ minute.

We adapt the CB algorithm to this delivery context while preserving its core principle: trigger a dispatch when accumulated waiting cost reaches a calibrated proportion of instantaneous matching cost. At each minute, the service provider evaluates whether to dispatch based on the balance between these two cost components. The waiting cost is defined as the elapsed time since the last dispatch times the number of drivers. This directly captures the reduction in remaining delivery commitment time: as waiting accumulates, the adjusted commitment time T_c shrinks, increasing the risk of delay. The matching cost is defined as the average delivery time per driver, which captures the expected delivery burden. Note that the average delivery time per order decreases as more orders accumulate, because routing efficiency improves with denser order distributions (drivers can serve multiple nearby locations in a single trip). This causes the matching cost to

decrease over time as the system accumulates more orders and drivers, mirroring the decreasing matching cost function $f(\mathbf{x})$ in Assumption 1. We justify the monotonicity property under this on-demand delivery scenario in Appendix EC.1.6. A dispatch is triggered when accumulated waiting cost exceeds α times the current matching cost, where α is a tunable parameter calibrated on training data. The pseudocode for this adapted algorithm is provided in Appendix EC.1.3.

We compare the CB algorithm against four benchmark policies: (1) Greedy, which dispatches immediately when both pools are non-empty; (2) Time Threshold, which dispatches after a fixed waiting time; (3) Quantity Threshold, which dispatches when the smaller pool exceeds a fixed size; and (4) Cost-Based Z-Threshold (Gautam and Geunes 2024), which dispatches when the sum of accumulated waiting and delivery costs exceeds a threshold Z . We also include the Practice policy, which reflects the actual batching strategy used by the platform.

For travel time estimation, we consider two approaches. The traveling salesman problem (TSP)-based approach computes optimal routes using a calibrated travel time matrix. The Travel Time Predictor Model, trained on actual delivery data following Liu et al. (2021), provides more realistic estimates by capturing driver behavior that deviates from planned routes. The rationale of adopting these two estimation approaches is discussed in Appendix EC.1.4.

7.2.3. Results and Discussion We evaluate policy performance on the test set (179 batches). To ensure a fair comparison, all policy parameters are calibrated via grid search on the training set, so that each benchmark operates at its best possible configuration. This approach avoids cherry-picking and ensures that performance differences reflect fundamental algorithmic advantages rather than suboptimal tuning. Details of the parameter calibration procedure are provided in Appendix EC.1.5.

Table 2 reports the average delay per driver in seconds under each policy, evaluated using both the TSP-based travel time estimates and the Predictor Model estimates.

Policy	TSP	Predictor Model
Greedy	76.76	283.52
Time Threshold	13.84	176.23
Quantity Threshold	4.52	122.83
Cost-Based Z-Threshold	31.84	174.85
CB	4.45	105.08
Practice		243.11

Table 2 Average Delay Comparison of CB Algorithm with Benchmark Policies

Several observations emerge from Table 2. First, the CB algorithm achieves the lowest average delay under both travel time estimation methods. Under the Predictor Model, which more accurately captures real-world

driver behavior, CB reduces average delay by 14.5% compared to the best fixed-rule benchmark (Quantity Threshold) and by 56.8% compared to the Practice policy actually implemented by the platform.

Second, the ranking of policies differs substantially between TSP and Predictor Model estimates. Under TSP, the Quantity Threshold and CB policies perform similarly well. Under the Predictor Model, the gap between CB and all other policies widens considerably. This discrepancy arises because TSP assumes drivers follow optimal routes, while in reality drivers deviate based on route familiarity, traffic conditions, and personal preferences. The Predictor Model captures these behavioral patterns, making it a more reliable basis for policy evaluation. The fact that CB maintains its advantage under the more realistic Predictor Model suggests that its performance gains are robust to modeling assumptions.

Table 3 reports average delivery time per order in seconds, which includes both the waiting time before dispatch and the actual delivery time after dispatch.

Policy	TSP	Predictor Model
Greedy	359.26	361.04
Time Threshold	402.41	361.35
Quantity Threshold	365.62	337.14
Cost-Based Z-Threshold	425.24	394.13
CB	367.25	331.41
Practice		476.79

Table 3 Average Delivery Time Comparison of CB Algorithm with Benchmark Policies

The CB algorithm achieves the lowest average delivery time under the Predictor Model (331.41 seconds) and remains competitive under TSP (367.25 seconds). This result complements the delay analysis: CB not only reduces violations of delivery commitments but also improves overall delivery efficiency. The improvement stems from CB's ability to adaptively balance batch sizes. When order and driver pools are thin, CB waits to accumulate more agents, capturing routing efficiency gains. When pools become thick, CB dispatches promptly to avoid excessive pre-dispatch waiting. This dynamic adjustment prevents the extreme batch sizes that would either sacrifice routing efficiency (too small) or overload drivers and extend delivery times (too large).

Among the fixed-rule benchmarks, the Quantity Threshold policy performs best on both metrics. This makes it the most relevant baseline for understanding CB's contribution. Figure 2 provides a detailed comparison between CB and Quantity Threshold across multiple performance dimensions, estimated using the Travel Time Predictor Model.

The comparison reveals that CB's advantages extend beyond average performance to tail-risk metrics. The CB algorithm achieves a 13.1% reduction in delay occurrences (the number of batches with at least one delayed delivery) and a 3.0% decrease in overall delay rate (the fraction of total deliveries that are delayed). In

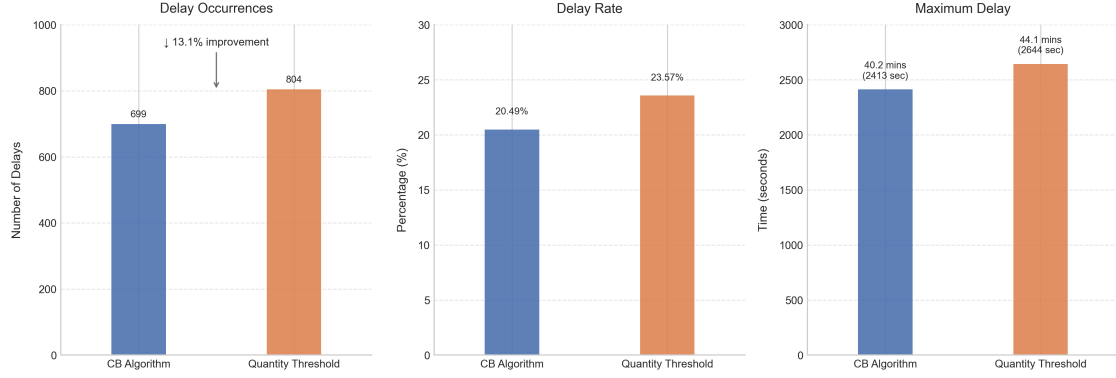


Figure 2 Performance Comparison: CB Algorithm vs Quantity Threshold

addition, the maximum delay under CB is 40.2 minutes, compared to 44.1 minutes under Quantity Threshold, representing a 9% improvement in worst-case performance. These tail-risk improvements are particularly valuable in delivery operations, where extreme delays damage customer satisfaction and platform reputation disproportionately.

Figure 3 compares CB with the Cost-Based Z-Threshold policy proposed by [Gautam and Geunes \(2024\)](#), estimated using the Travel Time Predictor Model. This comparison is particularly instructive because both policies use cost information, but in fundamentally different ways.

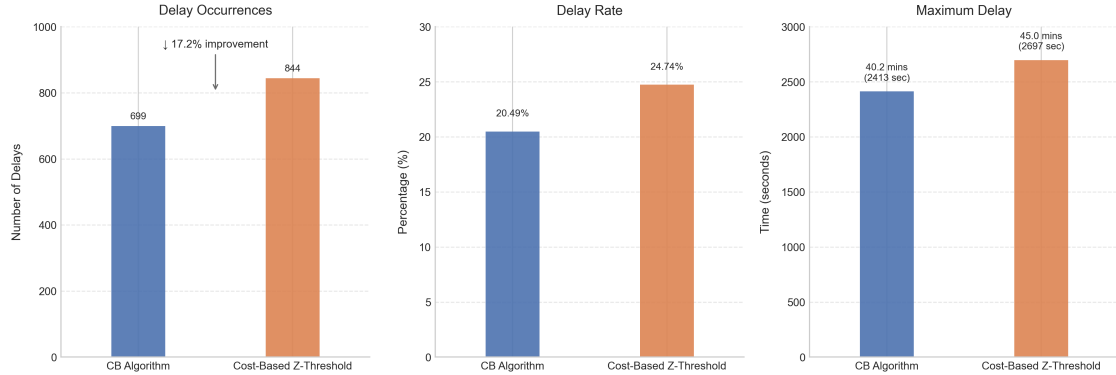


Figure 3 Performance Comparison: CB Algorithm vs Cost-Based Z-Threshold

The CB algorithm achieves a 17.2% reduction in delay occurrences compared to Z-Threshold. The key difference lies in how the two policies aggregate cost information. The Z-Threshold policy dispatches when the sum of accumulated waiting cost and current matching cost exceeds a fixed threshold Z . This additive approach treats waiting and matching costs as substitutes: a high matching cost can trigger dispatch even when waiting cost is low, and vice versa. In contrast, CB uses a ratio-based trigger, dispatching when waiting cost exceeds α times matching cost. This multiplicative approach treats the two costs as complements that must be balanced.

The ratio-based approach is more effective because it responds appropriately to the evolving cost structure. Consider two scenarios. In the first scenario, matching cost is initially high because the driver pool is thin. Under Z-Threshold, the high matching cost may push the sum above Z , triggering a premature dispatch before sufficient batching efficiency is achieved. Under CB, the ratio W/M remains low because waiting cost has not yet accumulated, so CB waits. In the second scenario, matching cost drops quickly because drivers arrive rapidly. Under Z-Threshold, the falling matching cost means the sum may remain below Z for an extended period, causing unnecessary waiting. Under CB, as matching cost falls, the ratio W/M rises, eventually triggering dispatch. In both scenarios, CB's ratio-based mechanism adapts more appropriately to the system dynamics.

8. Conclusion

Dynamic matching systems across domains face a fundamental tension between immediate action and strategic waiting. This paper develops a principled approach to resolving this tension through the cost-balancing principle, which triggers matching when accumulated waiting cost reaches a calibrated proportion of instantaneous matching cost.

8.1. Summary and Key Contributions

We conclude by summarizing the key contributions of this study. First, we develop the Cost-Balancing algorithm, a simple, adaptive policy that requires no distributional assumptions, no demand forecasting, and minimal parameter tuning. The algorithm's design is grounded in fluid limit analysis of the optimal policy, which reveals that the optimal matching decision is characterized by a cost ratio condition. This theoretical foundation ensures that the algorithm's simplicity does not come at the expense of principled design. Second, we establish rigorous performance guarantees for the CB algorithm. We prove that the algorithm achieves a competitive ratio of $(1 + \sqrt{\Gamma})$ under adversarial arrivals, where Γ quantifies the economies of scale in the matching cost function. This guarantee holds regardless of the arrival pattern, providing robustness against demand volatility and non-stationarity. In contrast, we show that standard heuristics, including greedy matching and fixed-threshold policies, can incur unbounded costs in worst-case scenarios. We further establish a universal lower bound of $(\sqrt{5} + 1)/2$ (the golden ratio) on the competitive ratio achievable by any online algorithm, demonstrating that our algorithm's performance is within a modest factor of the theoretical optimum. Third, we analyze the general attribute-based matching model and establish fundamental impossibility results. We prove that computing optimal policies is NP-hard for multi-sided markets with three or more agent types, and that no online algorithm can achieve bounded competitive ratios when the adversary controls both arrival times and agent attributes. These results characterize fundamental barriers of the attribute-based model, motivating the queue-based abstraction as a tractable alternative for achieving robust performance guarantees. Fourth, we demonstrate the algorithm's practical effectiveness through extensive experiments on game matchmaking and real-world food delivery data. The CB algorithm

consistently outperforms industry-standard heuristics across diverse market conditions, with improvements ranging from 1.6% to 6.2% in gaming and up to 56.8% in delivery operations compared to practice policies. A key advantage of our approach is its self-tuning nature: the algorithm adapts automatically to changing demand patterns without requiring manual recalibration, making it immediately deployable in practice.

8.2. Practical Implications

Our work offers several practical implications for platform operators. The CB algorithm provides a principled alternative to ad hoc batching heuristics that are widely used in industry. Unlike fixed time windows or queue-length thresholds that require careful calibration and frequent adjustment, the cost-balancing mechanism responds directly to realized system costs, eliminating the need for demand forecasting or parameter recalibration when market conditions change. The algorithm's computational simplicity is another practical advantage. Implementation requires only tracking queue lengths and a running sum of waiting costs, with no need for complex optimization or machine learning models. This simplicity facilitates integration into existing platform infrastructure and enables real-time decision-making at scale. Our numerical experiments demonstrate that the cost-balancing principle generalizes beyond the stylized assumptions of our theoretical model. In the gaming experiment, matching costs depend on continuous skill ratings rather than queue lengths; in the delivery experiment, matching involves one-to-many assignment with geographic routing constraints. The algorithm's strong performance in both settings suggests that the cost-balancing principle captures a fundamental insight about dynamic matching that extends to a broad class of applications.

8.3. Limitations and Future Research

This study opens several promising directions for future research. First, our model assumes that agents wait indefinitely until matched. In many real-world settings, agents may abandon the system if waiting times become excessive. Extending the cost-balancing framework to incorporate abandonment dynamics would enhance its applicability to impatient customer populations. Second, while we establish that the parameter $\alpha = \sqrt{\Gamma}$ yields the best competitive ratio guarantee, the optimal parameter may differ in specific stochastic environments. Future work could develop learning-based approaches to adaptively tune the balancing parameter based on observed system performance, potentially achieving better average-case performance while maintaining worst-case guarantees. Finally, our analysis focuses on a single matching pool where all agents of each type are compatible. Many practical applications involve compatibility constraints, geographic restrictions, or heterogeneous agent preferences that partition the market into overlapping sub-pools. Extending the cost-balancing principle to such structured matching markets represents a natural direction for future research.

References

Afeche P, Caldentey R, Gupta V (2022) On the optimal design of a bipartite matching queueing system. *Operations Research* 70(1):363–401.

Akbarpour M, Li S, Gharan SO (2020) Thickness and information in dynamic matching markets. *Journal of Political Economy* 128(3):783–815.

Aouad A, Saritaç Ö (2022) Dynamic stochastic matching under limited time. *Operations Research* 70(4):2349–2383.

Ashlagi I, Burq M, Dutta C, Jaillet P, Saberi A, Sholley C (2019) Edge weighted online windowed matching. *Proceedings of the 2019 ACM Conference on Economics and Computation*, 729–742.

Ashlagi I, Nikzad A, Strack P (2023) Matching in dynamic imbalanced markets. *The Review of Economic Studies* 90(3):1084–1124.

Ashlagi I, Roth AE (2021) Kidney exchange: An operations perspective. *Management Science* 67(9):5455–5478.

Baccara M, Lee S, Yariv L (2020) Optimal dynamic matching. *Theoretical Economics* 15(3):1221–1278.

Bahmani B, Kapralov M (2010) Improved bounds for online stochastic matching. *European Symposium on Algorithms*, 170–181 (Springer).

Balkanski E, Faenza Y, Périvier N (2023) The power of greedy for online minimum cost matching on the line. *Proceedings of the 24th ACM Conference on Economics and Computation*, 185–205.

Bhimaraju A, Etesami SR, Varshney LR (2026) Dynamic batching of online arrivals to leverage economies of scale. *European Journal of Operational Research* 328(3):749–761.

Blanchet JH, Reiman MI, Shah V, Wein LM, Wu L (2022) Asymptotically optimal control of a centralized dynamic matching market with general utilities. *Operations Research* 70(6):3355–3370.

Chen M, Elmachtoub AN, Lei X (2025a) Matchmaking strategies for maximizing player engagement in video games. *Management Science* Forthcoming.

Chen M, Hu M (2024) Courier dispatch in on-demand delivery. *Management Science* 70(6):3789–3807.

Chen Y, Kanoria Y, Kumar A, Zhang W (2025b) Feature-based dynamic matching. *Operations Research* .

Eom M, Toriello A (2025) Batching and greedy policies: How good are they in dynamic matching? *Manufacturing & Service Operations Management* .

Feldman J, Mehta A, Mirrokni V, Muthukrishnan S (2009) Online stochastic matching: Beating 1-1/e. *2009 50th Annual IEEE Symposium on Foundations of Computer Science*, 117–126 (IEEE).

Feng Y, Niazadeh R (2025) Batching and optimal multistage bipartite allocations. *Management Science* 71(5):4108–4130.

Feng Y, Niazadeh R, Saberi A (2024) Two-stage stochastic matching and pricing with applications to ride hailing. *Operations Research* 72(4):1574–1594.

Gan Y (2023) *Essays on dynamic optimization for markets and networks* (Columbia University).

Gautam N, Geunes J (2024) Analysis of real-time order fulfillment policies: When to dispatch a batch? *Service Science* 16(2):85–106.

Goyal V, Udwani R (2023) Online matching with stochastic rewards: Optimal competitive ratio via path-based formulation. *Operations Research* 71(2):563–580.

Gupta V (2024) Greedy algorithm for multiway matching with bounded regret. *Operations Research* 72(3):1139–1155.

Gurvich I, Ward A (2015) On the dynamic control of matching queues. *Stochastic Systems* 4(2):479–523.

Huang Z, Zhang Q (2020) Online primal dual meets online matching with stochastic rewards: configuration lp to the rescue. *Proceedings of the 52nd Annual ACM SIGACT Symposium on Theory of Computing*, 1153–1164.

Immorlica N, Lucier B, Manshadi V, Wei A (2023) Designing approximately optimal search on matching platforms. *Management Science* 69(8):4609–4626.

Jaillet P, Lu X (2014) Online stochastic matching: New algorithms with better bounds. *Mathematics of Operations Research* 39(3):624–646.

Kanoria Y (2025) Dynamic spatial matching. *The Annals of Applied Probability* 35(5):3086–3118.

Karp RM (1972) Reducibility among combinatorial problems. *Complexity of Computer Computations*, 85–103 (Springer).

Karp RM, Vazirani UV, Vazirani VV (1990) An optimal algorithm for on-line bipartite matching. *Proceedings of the twenty-second annual ACM symposium on Theory of computing*, 352–358.

Kerimov S, Ashlagi I, Gurvich I (2024) Dynamic matching: Characterizing and achieving constant regret. *Management Science* 70(5):2799–2822.

Kerimov S, Ashlagi I, Gurvich I (2025) On the optimality of greedy policies in dynamic matching. *Operations Research* 73(1):560–582.

Keskin NB, Scott J, Swinney R (2024) Order stacking in on-demand delivery platforms. *Working paper* URL <http://dx.doi.org/10.2139/ssrn.4947698>.

Kohlenberg A, Gurvich I (2025) The cost of impatience in dynamic matching: Scaling laws and operating regimes. *Management Science* 71(4):3303–3319.

Kuhn HW (1955) The hungarian method for the assignment problem. *Naval Research Logistics Quarterly* 2(1-2):83–97.

Liang H, Wang Z, Xu Y (2025) Spatial matching of random samples on a circle: Theoretic analysis and applications to ride-hailing systems. *Working paper* URL <http://dx.doi.org/10.2139/ssrn.5360747>.

Liu S, He L, Max Shen ZJ (2021) On-time last-mile delivery: Order assignment with travel-time predictors. *Management Science* 67(7):4095–4119.

Loertscher S, Muir EV, Taylor PG (2022) Optimal market thickness. *Journal of Economic Theory* 200:105383.

Ma H, Ma W, Romero M (2025) Potential-based greedy matching for dynamic delivery pooling. *Working paper* URL <http://dx.doi.org/10.48550/arXiv.2502.16862>.

Manshadi VH, Gharan SO, Saberi A (2012) Online stochastic matching: Online actions based on offline statistics. *Mathematics of Operations Research* 37(4):559–573.

Mehta A, Panigrahi D (2012) Online matching with stochastic rewards. *2012 IEEE 53rd annual symposium on foundations of computer science*, 728–737 (IEEE).

Mehta A, et al. (2013) Online matching and ad allocation. *Foundations and Trends® in Theoretical Computer Science* 8(4):265–368.

Mertikopoulos P, Nax HH, Pradelski BS (2024) Quick or cheap? breaking points in dynamic markets. *Journal of Mathematical Economics* 112:102987.

Uber (2023) How does uber match riders with drivers? <https://www.uber.com/us/en/marketplace/matching>.

Wang G, Zhang H, Zhang J (2024) On-demand ride-matching in a spatial model with abandonment and cancellation. *Operations Research* 72(3):1278–1297.

Wei L, Kapuscinski R, Jasin S (2021) Shipping consolidation across two warehouses with delivery deadline and expedited options for e-commerce and omni-channel retailers. *Manufacturing & Service Operations Management* 23(6):1634–1650.

Wei Y, Xu J, Yu SH (2023) Constant regret primal-dual policy for multi-way dynamic matching. *Working paper* URL <http://dx.doi.org/10.2139/ssrn.4357216>.

Xie Y, Ma W, Xin L (2025) The benefits of delay to online decision making. *Management Science* .

Zhao Y, Papier F, Teo CP (2024) Market thickness in online food delivery platforms: The impact of food processing times. *Manufacturing & Service Operations Management* 26(3):853–872.

E-Companion of “The Cost-Balancing Principle for Dynamic Matching Markets”

EC.1. Omitted Experiment Details of Section 7.2

This section provides additional implementation details for the delivery experiment in Section 7.2. We begin by formulating the underlying vehicle routing problem in Section EC.1.1 and describing its computational implementation in Section EC.1.2, including the initial solution heuristic. We then explain how the Cost-Balancing algorithm is adapted to the dispatching context in Section EC.1.3 and discuss the travel time estimation methods used in the numerical study in Section EC.1.4. Finally, we present the parameter calibration procedure in Section EC.1.5 and empirically verify the monotonicity of the matching cost in Section EC.1.6.

EC.1.1. VRP Formulation

The order assignment problem in Section 7.2 is formulated as a vehicle routing problem (VRP) with capacity constraints. This subsection provides a detailed description of the formulation, including the meaning of each component.

Let \mathcal{I} denote the set of customer locations to be served in a given dispatch batch, and let \mathcal{K} denote the set of available drivers at the time of dispatch. Each location $i \in \mathcal{I}$ has an associated order quantity q_i , representing the number of meal boxes to be delivered to that location. Each driver $k \in \mathcal{K}$ has a capacity limit C , representing the maximum number of meal boxes the driver can carry in a single trip.

The decision variables are binary assignment variables $y_{ik} \in \{0, 1\}$ for each location-driver pair $(i, k) \in \mathcal{I} \times \mathcal{K}$. Specifically, $y_{ik} = 1$ if location i is assigned to driver k , and $y_{ik} = 0$ otherwise. The vector $\mathbf{y}_k = \{y_{ik}\}_{i \in \mathcal{I}}$ collects all assignment decisions for driver k , defining the set of locations $\mathcal{I}_k = \{i \in \mathcal{I} : y_{ik} = 1\}$ that driver k must visit.

The objective is to minimize the expected total delivery delay across all drivers. Because service times at customer locations are uncertain (depending on factors such as customer availability and order complexity), we adopt a sample average approximation (SAA) approach. Let \mathcal{S} denote a set of scenarios, where each scenario $s \in \mathcal{S}$ specifies a realization of service times $\{t_i^s\}_{i \in \mathcal{I}}$.

For a given assignment, driver k ’s total delivery time consists of two components: (1) the sum of service times at assigned locations, $\sum_{i \in \mathcal{I}} t_i^s y_{ik}$, and (2) the travel time l_k required to visit all assigned locations and return to the depot. The travel time $l_k = l(\mathbf{y}_k)$ is determined by solving a TSP over the assigned locations, finding the shortest route that starts at the depot, visits all locations in \mathcal{I}_k , and returns to the depot.

Driver k ’s delay in scenario s is the positive part of the difference between total delivery time and the commitment time T_c :

$$\left(\sum_{i \in \mathcal{I}} t_i^s y_{ik} + l_k - T_c \right)^+.$$

The objective function averages this delay across all drivers and scenarios:

$$\frac{1}{|\mathcal{S}| \cdot |\mathcal{K}|} \sum_{s \in \mathcal{S}} \sum_{k \in \mathcal{K}} \left(\sum_{i \in \mathcal{I}} t_i^s y_{ik} + l_k - T_c \right)^+$$

The formulation includes three types of constraints:

1. Coverage constraint: Each location must be served by exactly one driver.

$$\sum_{k \in \mathcal{K}} y_{ik} = 1, \quad \forall i \in \mathcal{I}.$$

This ensures that every customer order is delivered and that no location is visited by multiple drivers.

2. Capacity constraint: The total order quantity assigned to each driver must not exceed the driver's capacity.

$$\sum_{i \in \mathcal{I}} q_i y_{ik} \leq C, \quad \forall k \in \mathcal{K}.$$

This reflects the physical limitation that each driver can carry at most C meal boxes.

3. Routing constraint: The travel time for each driver is determined by the TSP solution over assigned locations.

$$l_k = l(\mathbf{y}_k), \quad \forall k \in \mathcal{K}.$$

This constraint couples the assignment decisions with the routing subproblem. In practice, we solve the TSP for each driver's assigned locations to compute l_k .

Combining the objective and constraints, the VRP formulation is:

$$\begin{aligned} \min_{y_{ik}} \quad & \frac{1}{|\mathcal{S}| |\mathcal{K}|} \sum_{s \in \mathcal{S}} \sum_{k \in \mathcal{K}} \left(\sum_{i \in \mathcal{I}} t_i^s y_{ik} + l_k - T_c \right)^+ \\ \text{s.t.} \quad & \sum_{k \in \mathcal{K}} y_{ik} = 1, \quad \forall i \in \mathcal{I}, \\ & \sum_{i \in \mathcal{I}} q_i y_{ik} \leq C, \quad \forall k \in \mathcal{K}, \\ & l_k = l(\mathbf{y}_k), \quad \forall k \in \mathcal{K}, \\ & y_{ik} \in \{0, 1\}, \quad \forall i \in \mathcal{I}, k \in \mathcal{K}. \end{aligned} \tag{EC.1}$$

This formulation is a mixed-integer nonlinear program due to the positive-part operator in the objective and the TSP subproblem embedded in the routing constraint. We solve it using Gurobi with linearization techniques for the positive-part operator and a callback mechanism to compute TSP travel times. Implementation details are provided in Section EC.1.2.

EC.1.2. VRP Optimization Implementation

This subsection provides details on the computational implementation of the VRP formulation described in Section EC.1.1.

The VRP optimization was conducted using Gurobi Optimizer version 11.0.0 build v11.0.0rc2 (win64 - Windows 11+0 (22631.2)). Computations were performed on an AMD Ryzen 5 5600G with Radeon Graphics processor featuring 6 physical cores and 12 logical processors, utilizing up to 12 parallel threads. Following the methodology established in [Liu et al. \(2021\)](#), we implemented termination criteria of either 20 minutes of computation time or achievement of a MIP gap less than 0.01, which proved sufficient to obtain near-optimal solutions.

To enhance solution quality and computational efficiency, we developed a specialized initial solution construction heuristic. This heuristic addresses the nontrivial case where the number of orders exceeds the number of available drivers, which is common in delivery operations during peak periods.

The heuristic operates in two phases. In Phase 1, we initialize the assignment by distributing drivers to geographically dispersed locations. For each driver, we identify and assign the order whose location is maximally distant from both the depot and all currently assigned order locations. This strategy maximizes spatial coverage and ensures that drivers are initially positioned to serve orders across the service area. Mathematically, for each driver k , we select order $i^* = \operatorname{argmax}_{i \in \mathcal{I} \setminus \mathcal{A}} \min_{j \in \mathcal{A} \cup \{\text{depot}\}} d(i, j)$, where \mathcal{A} denotes the set of already assigned orders and $d(i, j)$ is the travel time between locations i and j . After Phase 1, each driver has exactly one order assigned, and we update each driver's current position and total travel time accordingly.

In Phase 2, we iteratively assign the remaining unassigned orders. At each iteration, we identify the driver with the minimum total travel time and assign to this driver the nearest unassigned order that satisfies the capacity constraint. This greedy strategy balances the workload across drivers while minimizing incremental travel time. The process continues until all orders are assigned or no feasible assignment exists.

The underlying principle of this heuristic is twofold: initially distributing drivers to geographically dispersed locations to maximize coverage, then systematically balancing total travel time by assigning orders to drivers with minimal incremental cost. This approach not only establishes a performance floor for our VRP solution but also significantly accelerates convergence to near-optimal solutions.

To illustrate the effectiveness of our developed heuristic, we present a complex test case involving 25 drivers and 154 orders. The corresponding VRP formulation contains 3,900 continuous variables, 604,500 binary variables, and 608,580 constraints, representing a computational challenge of considerable scale.

Table EC.1 compares the computational performance of the standard Gurobi approach with our heuristic-based initialization. Without our heuristic, Gurobi reaches the 20-minute time limit with a suboptimal objective value of 55,360.38, demonstrating the difficulty of this large-scale optimization problem. In contrast, our heuristic generates an initial feasible solution with an objective value of 4,347.8 in under 1

Algorithm 2 Initial Solution Construction Heuristic

Require: Order set \mathcal{I} , Driver set \mathcal{K} , Travel time function $d(i, j)$, Depot location, Capacity limit C , Order quantities $\{q_i\}_{i \in \mathcal{I}}$

Ensure: Initial feasible assignment \mathcal{A} with driver positions and travel times

```
1:  $\mathcal{A} \leftarrow \emptyset$                                 ▷ Initialize assigned orders
2: Initialize driver positions:  $\text{pos}(k) \leftarrow \text{depot}$  for all  $k \in \mathcal{K}$ 
3: Initialize driver travel times:  $t_k \leftarrow 0$  for all  $k \in \mathcal{K}$ 
4: Initialize driver loads:  $\text{load}(k) \leftarrow 0$  for all  $k \in \mathcal{K}$ 

Phase 1: Initial Distribution

5: for each driver  $k \in \mathcal{K}$  do
6:   Find order  $i^* = \text{argmax}_{i \in \mathcal{I} \setminus \mathcal{A}} \min_{j \in \mathcal{A} \cup \{\text{depot}\}} d(i, j)$ 
7:   Assign  $i^*$  to driver  $k$ :  $\mathcal{A} \leftarrow \mathcal{A} \cup \{i^*\}$ 
8:   Update driver  $k$ 's position:  $\text{pos}(k) \leftarrow i^*$ 
9:   Update driver  $k$ 's travel time:  $t_k \leftarrow d(\text{depot}, i^*)$ 
10:  Update driver  $k$ 's load:  $\text{load}(k) \leftarrow q_{i^*}$ 
11: end for
```

Phase 2: Remaining Order Assignment

```
12: while  $\mathcal{A} \neq \mathcal{I}$  do
13:   Find driver  $k^* = \text{argmin}_{k \in \mathcal{K}} t_k$ 
14:   Find feasible nearest order:  $i_{\text{nearest}} = \text{argmin}_{i \in \mathcal{I} \setminus \mathcal{A}: \text{load}(k^*) + q_i \leq C} d(\text{pos}(k^*), i)$ 
15:   if  $i_{\text{nearest}}$  does not exist then
16:     break                                ▷ No feasible assignment possible
17:   end if
18:   Assign  $i_{\text{nearest}}$  to driver  $k^*$ :  $\mathcal{A} \leftarrow \mathcal{A} \cup \{i_{\text{nearest}}\}$ 
19:   Update driver  $k^*$ 's travel time:  $t_{k^*} \leftarrow t_{k^*} + d(\text{pos}(k^*), i_{\text{nearest}})$ 
20:   Update driver  $k^*$ 's position:  $\text{pos}(k^*) \leftarrow i_{\text{nearest}}$ 
21:   Update driver  $k^*$ 's load:  $\text{load}(k^*) \leftarrow \text{load}(k^*) + q_{i_{\text{nearest}}}$ 
22: end while
23: return Initial feasible assignment with driver positions and travel times
```

second. Using this solution as a starting point, Gurobi then converges to a near-optimal solution with an objective value of 624.83 in just 80 seconds, representing a 98.9% improvement over the standard approach and a significant reduction in computational time.

Method	Initial Solution Objective Value	Initial Time (seconds)	Final Solution Objective Value	Total Time (seconds)
Standard Gurobi	N/A	N/A	55,360.38	1,200
Our Heuristic + Gurobi	4,347.8	< 1	624.83	80
Improvement	—	—	98.9%	93.3%

Table EC.1 Computational Performance Comparison for VRP Instance (25 drivers, 154 orders)

Note: The standard Gurobi approach reached the 20-minute time limit without finding a good solution. Our heuristic provides a high-quality starting point that enables rapid convergence to near-optimality.

EC.1.3. CB Algorithm Adaptation

We adapt the Cost-Balancing algorithm to the delivery dispatch setting while preserving its core principle: trigger a dispatch when accumulated waiting cost reaches a calibrated proportion of instantaneous matching cost. The adaptation requires specifying how to measure waiting cost and matching cost in the delivery context, as well as how to implement the cost-balancing condition.

In the base model (Section 3), waiting cost accumulates at rate $\sum_i c_i X_i(t)$, where $X_i(t)$ is the queue length of type i . In the delivery setting, we simplify this to focus on the time dimension. The waiting cost is defined as

$$\text{Waiting Cost} = |\mathcal{K}| \cdot W,$$

where $|\mathcal{K}|$ is the number of available drivers and W is the elapsed time (in minutes) since the last dispatch. This formulation captures the reduction in remaining delivery commitment time: as waiting accumulates, the adjusted commitment time $T_c = T_0 - W$ shrinks, increasing the risk of delay. Multiplying by the number of drivers reflects that more drivers waiting implies greater urgency to dispatch.

The matching cost captures the expected delivery burden per driver given the current order and driver pools. We define it as the average delivery time per driver:

$$M = \frac{1}{|\mathcal{K}|} \sum_{k \in \mathcal{K}} \left(\sum_{i \in \mathcal{I}_k} \tilde{t}_i + l_k(\mathcal{I}_k) \right),$$

where \tilde{t}_i is the service time at location i and $l_k(\mathcal{I}_k)$ is the travel time for driver k given assignment \mathcal{I}_k . The intuition behind this formulation is twofold. First, the average delivery time per order typically decreases as more orders accumulate, because routing efficiency improves with denser order distributions. Second, the ratio of orders to drivers reflects traffic intensity: a higher ratio suggests more efficiency gain per driver from batching. Thus, the matching cost tends to decrease over time as the system accumulates more orders and drivers, mirroring the decreasing cost function $f(\mathbf{x})$ in Assumption 1.

The CB algorithm triggers a dispatch when the waiting cost exceeds α times the matching cost:

$$|\mathcal{K}| \cdot W > \alpha M.$$

This condition shows that the effective threshold adapts to the number of available drivers. When more drivers are available, the algorithm dispatches sooner (lower effective threshold), preventing excessive idle time. When fewer drivers are available, the algorithm waits longer to accumulate orders for better routing efficiency.

Algorithm 3 presents the complete pseudocode for the adapted CB algorithm. The algorithm operates in discrete time steps of $\Delta t = 1$ minute, evaluating the dispatch decision at each step.

Algorithm 3 Cost-Balancing Algorithm for Delivery Dispatch

Require: Time horizon T , time step Δt , scaling factor α

Ensure: Dispatch timestamps \mathcal{D}

```
1:  $t \leftarrow 0$ ,  $\mathcal{D} \leftarrow \emptyset$ ,  $W \leftarrow 0$ 
2:  $\mathcal{I} \leftarrow \emptyset$                                 ▷ Current pool of undelivered orders
3:  $\mathcal{K} \leftarrow \emptyset$                             ▷ Current pool of available drivers
4: while  $t < T$  do
5:    $t \leftarrow t + \Delta t$ 
6:   Update  $\mathcal{I}$  with new orders arriving in  $(t - \Delta t, t]$ 
7:   Update  $\mathcal{K}$  with new drivers becoming available in  $(t - \Delta t, t]$ 
8:   if  $|\mathcal{K}| = 0$  or  $|\mathcal{I}| = 0$  then
9:     continue                                ▷ No feasible dispatch
10:    end if
11:     $W \leftarrow W + \Delta t$                       ▷ Waiting time increment
12:    Compute dispatch plan and obtain the current matching cost  $M$ 
13:    if  $|\mathcal{K}| \cdot W > \alpha M$  then
14:       $\mathcal{D} \leftarrow \mathcal{D} \cup \{t\}$                   ▷ Record dispatch time
15:       $\mathcal{I} \leftarrow \emptyset$ ,  $\mathcal{K} \leftarrow \emptyset$           ▷ Remove dispatched orders and drivers
16:       $W \leftarrow 0$                                 ▷ Reset waiting clock after dispatch
17:    end if
18:  end while
19: return  $\mathcal{D}$ 
```

Lines 1–3 initialize the system state: the current time t , the set of dispatch timestamps \mathcal{D} , the waiting time counter W , and the order and driver pools \mathcal{I} and \mathcal{K} . The main loop (Lines 4–16) processes each time step. At each step, the algorithm first updates the pools with newly arrived orders and drivers (Lines 6–7). If either pool is empty, dispatch is infeasible and the algorithm continues to the next time step (Lines 8–9). Otherwise, the waiting time counter increments (Line 10), and the algorithm computes the current matching

cost by solving the VRP formulation (Line 11). The cost-balancing condition is then evaluated (Line 12). If the condition is satisfied, a dispatch is triggered: the current time is recorded, the pools are cleared, and the waiting counter resets (Lines 13–15). After processing all time steps, the algorithm returns the sequence of dispatch timestamps.

EC.1.4. Discussion on Travel Time Estimation Methods

In the experimental results, we observe notable discrepancies between the TSP-based and Predictor Model estimates, which warrant further discussion. Understanding these differences is important because the choice of travel time estimation method affects policy evaluation and the conclusions drawn about algorithmic performance.

The TSP routing approach, widely used in both academic literature and industry practice, provides a theoretically optimal delivery path with minimum total travel time. In our implementation, travel times between customer locations are estimated using a calibrated travel time matrix derived from Baidu Map’s RouteMatrix API. To account for the speeding effect from electric bikes commonly used by delivery drivers, we scale down the estimated travel time by a factor of 4/3, following the calibration approach in [Liu et al. \(2021\)](#).

However, as documented in [Liu et al. \(2021\)](#), real-world drivers often deviate from the theoretically optimal TSP routes. Their empirical analysis shows that actual delivery travel time is consistently greater than or equal to the TSP solution, with an average difference of 3.8 minutes and an average relative difference of 21%. Several factors contribute to this systematic deviation:

1. Practical road constraints: The TSP formulation does not account for real-world constraints such as limited left-turn flows at certain intersections, one-way streets, or restricted access zones that drivers must navigate around.
2. Driver routing preferences: Drivers may prefer certain travel patterns over others. For instance, zigzagging routes are often avoided due to increased accident risk on busy streets, even if they represent the shortest path.
3. Real-time adaptations: Drivers adjust their routes based on real-time traffic conditions, weather, and updated customer locations, leading to deviations from pre-planned sequences.
4. Route familiarity: Experienced drivers may have preferred routes through familiar neighborhoods that differ from the theoretically optimal path but are more efficient in practice due to local knowledge.

Given the difficulty of modeling all practical constraints and behavioral considerations in a mathematical formulation, we adopt a machine learning approach to predict travel time. Following [Liu et al. \(2021\)](#), we train a random forest model on the training set using features such as order quantity, route distance, and geographic characteristics (latitudinal and longitudinal differences between locations). This predictor model learns from actual delivery data to estimate driver travel times without requiring specification of the visiting sequence.

The Predictor Model captures the systematic gap between theoretical and actual travel times by implicitly learning driver behavior patterns from historical data. This approach is particularly valuable because it reflects the actual consequences of routing decisions rather than idealized assumptions.

The choice of travel time estimation method has important implications for policy comparison. Under TSP-based estimation, policies that trigger dispatch with larger batches benefit from the idealized routing assumption, as the theoretical efficiency gains from batching are fully realized. Under the Predictor Model, the gap between CB and other policies widens because the more realistic estimates reveal performance differences that are masked by TSP assumptions.

Specifically, with large batch sizes and heavy traffic, TSP tends to underestimate delivery time because the theoretical minimum-distance route does not account for the practical constraints that become more binding as complexity increases. Conversely, with small assignments, TSP may overestimate delivery time, as real-world drivers can leverage route familiarity and practical shortcuts.

The practice-implemented policy, which uses fixed 15-minute batching intervals, performs poorly. This can be attributed to two factors: inflexible dispatch timing that ignores the current system state, and potentially unbalanced order assignments that lead to large variations in delivery times among drivers.

Since our goal is to evaluate policies under realistic conditions, we consider the Predictor Model results as the primary basis for comparison, while reporting TSP results for completeness and comparability with other studies that use theoretical routing assumptions.

EC.1.5. Parameter Calibration

This subsection describes the parameter calibration procedure for all dispatch policies, including the search methodology, optimal parameter values, and interpretation of results. Our goal is to give each policy the best chance to perform well so that performance differences reflect algorithmic design rather than poor tuning.

To ensure a fair comparison across policies, we calibrate all parameters using grid search on the training set (716 batches). For each policy, we evaluate performance across a predefined parameter range and select the value that minimizes average delay on the training data. This approach avoids cherry-picking and ensures that each benchmark operates at its best possible configuration under our evaluation metric.

The grid search is conducted independently for each policy, using the same training-test split and evaluation metric (average delay per driver). All experiments use the Travel Time Predictor Model for consistency, as it provides more realistic estimates of driver behavior than idealized TSP routing (see Section EC.1.4).

Table EC.2 summarizes the search ranges, step sizes, and optimal values for each policy.

The optimal $\alpha = 0.5$ for the CB algorithm is not only empirically favorable but also supported by theoretical intuition. Specifically, the value aligns with an approximation method, where the waiting and matching costs are computed using expected values. In this approximation, the number of drivers is replaced by the optimal

Parameter	Search Range	Step	Optimal
Time Threshold	1–15 min	1 min	7 min
Quantity Threshold	1–10	1	3
Cost-Based Z-Threshold	20–35 min	1 min	32 min
α (CB)	0.1–1.0	0.1	0.5

Table EC.2 Parameter Calibration Results for Delivery Experiment

quantity threshold, the waiting cost is replaced by the optimal waiting time threshold, and the matching cost is estimated using the sample average of delivery time and order quantity.

$$\alpha \approx \frac{\text{average waiting cost}}{\text{average matching cost}} = \frac{7 * 60}{851.21} = 0.49.$$

Under this average-based approximation, the derived α value also approximates 0.5, providing a compelling theoretical justification for the empirical result.

The initial delivery commitment time T_0 is set at 35 minutes, which is slightly stricter than the 45-minute setting in [Liu et al. \(2021\)](#). This stricter commitment time simulates a high-load environment that better highlights the differences in algorithmic performance, as policies must operate closer to their capacity limits.

The travel time predictor model is trained on the 716 training batches using a random forest algorithm with features proposed by [Liu et al. \(2021\)](#). These attributes summarize both the scale and geometry of each batch of customer locations. For completeness, we include the feature table below.

Attribute	Definition
\bar{d}	Average distance between the depot and customer locations
d	Shortest distance between the depot and customer locations
D	Longest distance between the depot and customer locations
R	Area of the smallest rectangle covering the customer locations
R'	Area of the smallest rectangle covering both the depot and the customer locations
L	Area of the smallest lune (formed by two equal-angle sectors from the depot) covering the customer locations
a	Maximum latitudinal difference between a pair of customer locations
b	Maximum longitudinal difference between a pair of customer locations
a'	Maximum latitudinal difference between any two locations including the depot
b'	Maximum longitudinal difference between any two locations including the depot
cstdev_a	Standard deviation of latitudinal differences between the depot and customer locations
cstdev_b	Standard deviation of longitudinal differences between the depot and customer locations
s_a	Average latitudinal difference between pairs of customer locations
s_b	Average longitudinal difference between pairs of customer locations

Table EC.3 Graph-Based Attributes Used in the Travel Time Predictor Model

EC.1.6. Verification of Matching Cost Monotonicity

A key assumption underlying the CB algorithm is that the matching cost decreases as the queue length increases (Assumption 1). This monotonicity property is essential for the cost-balancing principle to function correctly: if matching costs did not decrease with queue length, there would be no benefit to waiting, and immediate dispatch would always be optimal. We verify this property empirically using 2,323 dispatch batches from our delivery experiment, sampled from the decision points of the optimally implemented CB algorithm with $\alpha = 0.5$.

We first examine how matching cost varies with the number of accumulated orders. In the delivery context, larger order pools enable more efficient routing: drivers can serve multiple nearby locations in a single trip, reducing travel time per order. Table EC.4 presents the grouped analysis by order quantity.

Order Range	Mean Orders	Sample Size	Avg Delivery Time (s)
1–12	6.9	1205	521.2
13–23	17.1	714	319.5
24–34	27.6	241	261.6
35–46	39.1	98	225.2
47–57	50.8	39	202.1
58–68	62.4	18	218.7
70–79	74.0	6	186.3

Table EC.4 Average Delivery Time by Order Quantity

The data reveals a clear decreasing trend: as the number of orders increases from 1–12 to 70–79, the average delivery time decreases from 521 seconds to 186 seconds, representing a 64.3% reduction. The corresponding simple linear regression is

$$\text{avg_delivery_time} = 560.81 - 10.00 \times \text{order_num},$$

indicating that each additional order reduces the average delivery time by approximately 10 seconds. This substantial improvement reflects the routing efficiency gains from denser order distributions.

We note a slight non-monotonicity in the 58–68 order range (218.7 seconds), which is higher than the adjacent 47–57 range (202.1 seconds). This deviation is likely due to limited sample size (only 18 observations) and the inherent variability in order locations. Despite this local fluctuation, the overall trend is clearly decreasing, and the regression captures the dominant relationship.

Using order quantity alone does not fully capture the system state, as the driver pool also affects matching efficiency. When more drivers are available, orders can be distributed more evenly, reducing the workload per driver. To capture the joint effect of order and driver accumulation, we analyze the relationship between waiting time and matching cost. As the system waits longer, both order and driver pools grow, and their interaction determines the actual matching cost.

Waiting Time (min)	Sample Size	Avg Delivery Time (s)	Avg Orders
1	489	531.9	7.2
2	608	435.1	13.6
3	570	388.9	18.4
4	366	344.4	19.0
5	173	302.7	19.2
6	68	267.2	20.0
7	31	247.6	18.4
8	14	224.0	22.1
9	4	195.5	20.0

Table EC.5 Average Delivery Time by Waiting Time

Table EC.5 shows that average delivery time decreases monotonically from 532 seconds at 1 minute of waiting to 195 seconds at 9 minutes, a 63.3% reduction. Unlike the order quantity analysis, the waiting time analysis exhibits strict monotonicity across all observed values. The corresponding regression is

$$\text{avg_delivery_time} = 554.33 - 51.13 \times \text{waiting_time},$$

indicating that each additional minute of waiting reduces the average delivery time by approximately 51 seconds. This larger coefficient (compared to 10 seconds per order) reflects that waiting time captures multiple effects simultaneously: more orders, more drivers, and better order-driver matching opportunities.

Figure EC.1 visualizes these relationships. The left panel shows the decreasing trend of average delivery time with order quantity, while the right panel demonstrates the monotonic decrease with waiting time. A notable feature of both curves is that the slope is steep at low values and gradually flattens as queue length or waiting time increases. This pattern reflects diminishing marginal returns: the benefit of adding one more agent or waiting one more minute is largest when the pool is small and decreases as more agents accumulate. In the left panel, as we can find from Table EC.4, moving from 7 to 17 orders reduces delivery time by approximately 200 seconds, while moving from 50 to 74 orders yields only about 16 seconds of improvement. Similarly, in the right panel, the first few minutes of waiting produce the largest gains.

This empirical pattern provides support for the convexity assumption used in Section 4.1, which requires that the matching cost function exhibits diminishing marginal returns. The observed curvature in Figure EC.1 suggests that the delivery setting satisfies these structural properties, lending empirical credibility to the theoretical analysis.

These results confirm that the matching cost function in the delivery setting satisfies the monotonicity property required by Assumption 1. The economies-of-scale effect arises from two complementary mechanisms: (1) routing efficiency, where denser order distributions enable shorter travel distances per delivery, and (2) load balancing, where larger driver pools allow more even distribution of orders across drivers. Together, these mechanisms create substantial benefits from waiting, which the CB algorithm exploits by

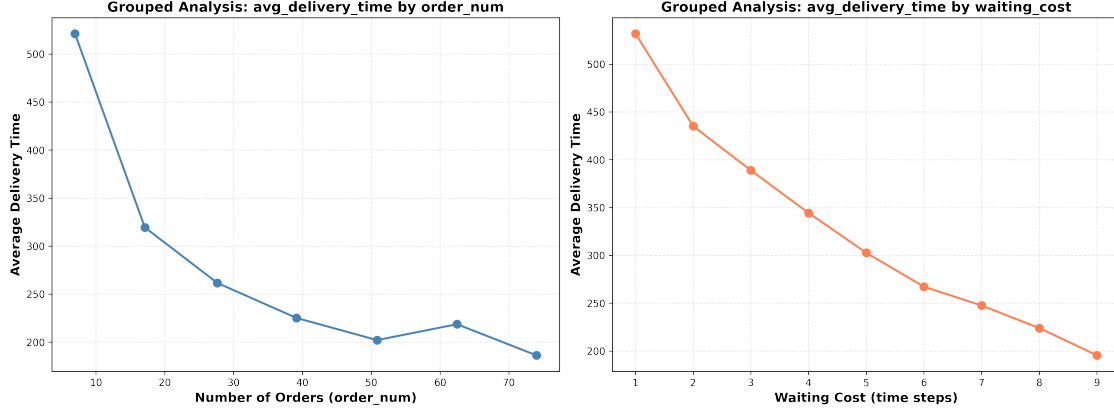


Figure EC.1 Empirical Verification of Matching Cost Monotonicity

delaying dispatch until the accumulated waiting cost justifies the current matching cost. The empirical verification provides confidence that the theoretical guarantees derived under Assumption 1 apply to practical delivery operations.

EC.2. Omitted Proofs of Section 4

EC.2.1. Proof of Proposition 1

To prove the proposition, we first establish the following technical lemma.

LEMMA EC.1. *If a function $f(\mathbf{x})$ is convex, supermodular, and component-wise non-increasing, then the function $g(\mathbf{x}) = f(\mathbf{x} + \mathbf{e}_i) - f(\mathbf{x})$ is non-decreasing for all \mathbf{x} and i .*

Proof of Lemma EC.1. We want to show that $g(\mathbf{x}) = f(\mathbf{x} + \mathbf{e}_i) - f(\mathbf{x})$ is non-decreasing in \mathbf{x} , i.e., $g(\mathbf{y}) \geq g(\mathbf{x})$ for all $\mathbf{y} \geq \mathbf{x}$. It suffices to show that $g(\mathbf{x} + \mathbf{e}_j) \geq g(\mathbf{x})$ for all j .

Case 1: $j = i$.

$$g(\mathbf{x} + \mathbf{e}_i) - g(\mathbf{x}) = [f(\mathbf{x} + 2\mathbf{e}_i) - f(\mathbf{x} + \mathbf{e}_i)] - [f(\mathbf{x} + \mathbf{e}_i) - f(\mathbf{x})].$$

From the convexity of f , we have $2f(\mathbf{x} + \mathbf{e}_i) \leq f(\mathbf{x}) + f(\mathbf{x} + 2\mathbf{e}_i)$, which implies $f(\mathbf{x} + 2\mathbf{e}_i) - f(\mathbf{x} + \mathbf{e}_i) \geq f(\mathbf{x} + \mathbf{e}_i) - f(\mathbf{x})$. Thus, $g(\mathbf{x} + \mathbf{e}_i) \geq g(\mathbf{x})$.

Case 2: $j \neq i$.

$$g(\mathbf{x} + \mathbf{e}_j) - g(\mathbf{x}) = [f(\mathbf{x} + \mathbf{e}_i + \mathbf{e}_j) - f(\mathbf{x} + \mathbf{e}_j)] - [f(\mathbf{x} + \mathbf{e}_i) - f(\mathbf{x})].$$

From the supermodularity of f , we have $f(\mathbf{x} + \mathbf{e}_i) + f(\mathbf{x} + \mathbf{e}_j) \leq f(\mathbf{x}) + f(\mathbf{x} + \mathbf{e}_i + \mathbf{e}_j)$, which implies $f(\mathbf{x} + \mathbf{e}_i + \mathbf{e}_j) - f(\mathbf{x} + \mathbf{e}_j) \geq f(\mathbf{x} + \mathbf{e}_i) - f(\mathbf{x})$. Thus, $g(\mathbf{x} + \mathbf{e}_j) \geq g(\mathbf{x})$.

Combining both cases, $g(\mathbf{x})$ is non-decreasing in \mathbf{x} . \square

We prove the monotonicity of the optimal policy by analyzing the structural properties of the value function in the corresponding dynamic programming formulation.

Consider the discrete-time approximation of the system (via uniformization with rate $\Lambda > \sum_{i=1}^N \lambda_i$), where at each decision epoch we choose between matching (action $a = 1$) and waiting (action $a = 0$). To establish this monotonicity rigorously, we work with value iteration. Let $J_k(\mathbf{x})$ denote the optimal k -stage cost function at iteration k , initialized with $J_0(\mathbf{x}) = 0$. We define the value iteration based on the Bellman operator as follows:

$$J(\mathbf{x}) = \min \left\{ \begin{array}{l} W(\mathbf{x}) := c(\mathbf{x}) + \sum_{i=1}^N \lambda_i J(\mathbf{x} + \mathbf{e}_i) + (1 - \Lambda) J(\mathbf{x}), \\ M(\mathbf{x}) := f(\mathbf{x}) + c(\mathbf{x} - \mathbf{1}) + \sum_{i=1}^N \lambda_i J(\mathbf{x} - \mathbf{1} + \mathbf{e}_i) + (1 - \Lambda) J(\mathbf{x} - \mathbf{1}) \end{array} \right\}. \quad (\text{EC.2})$$

From (EC.2), we can derive the following relationship:

$$M(\mathbf{x}) = f(\mathbf{x}) + W(\mathbf{x} - \mathbf{1}). \quad (\text{EC.3})$$

The net benefit of matching is $\Delta(\mathbf{x}) = W(\mathbf{x}) - M(\mathbf{x})$. Substituting terms and noting $c(\mathbf{x}) - c(\mathbf{x} - \mathbf{1}) = \sum c_i$ (constant), we have:

$$\Delta(\mathbf{x}) = \sum c_i - f(\mathbf{x}) + \mathcal{E}[J(\mathbf{x}) - J(\mathbf{x} - \mathbf{1})], \quad (\text{EC.4})$$

where \mathcal{E} is the expectation operator defined as

$$\mathcal{E}g(\mathbf{x}) = \sum \lambda_i g(\mathbf{x} + \mathbf{e}_i) + (1 - \Lambda) g(\mathbf{x}).$$

To prove the policy is monotone (i.e., match set is closed upwards), it suffices to show $\Delta(\mathbf{x})$ is non-decreasing in \mathbf{x} . Let $G_k(\mathbf{x}) = J_k(\mathbf{x}) - J_k(\mathbf{x} - \mathbf{1})$. Then

$$\Delta_k(\mathbf{x}) = \sum c_i - f(\mathbf{x}) + \mathcal{E}G_k(\mathbf{x}).$$

We proceed by induction on k to show two properties simultaneously:

1. $\Delta_k(\mathbf{x})$ is non-decreasing in \mathbf{x} (i.e., the optimal policy is of threshold type).
2. $G_k(\mathbf{x} + \mathbf{e}_i) - G_k(\mathbf{x}) \geq f(\mathbf{x} + \mathbf{e}_i) - f(\mathbf{x})$ for all \mathbf{x} .

Base Case ($k = 0$): $J_0(\mathbf{x}) = 0 \implies G_0(\mathbf{x}) = 0$.

- $\Delta_0(\mathbf{x}) = \sum c_i - f(\mathbf{x})$. Since $f(\mathbf{x})$ is non-increasing, $-f(\mathbf{x})$ is non-decreasing, so $\Delta_0(\mathbf{x})$ is non-decreasing.
- Since f is non-increasing, $f(\mathbf{x} + \mathbf{e}_i) \leq f(\mathbf{x})$, so

$$G_0(\mathbf{x} + \mathbf{e}_i) - G_0(\mathbf{x}) = 0 \geq f(\mathbf{x} + \mathbf{e}_i) - f(\mathbf{x}).$$

The inequality holds.

Inductive Step: Assume properties (i) and (ii) hold for k . Property (i) for k implies that for any k , there exists a boundary separating the Wait and Match regions such that we Match if \mathbf{x} is “large enough”. We first analyze $G_{k+1}(\mathbf{x})$ to prove (ii) for $k + 1$. Recall $J_{k+1}(\mathbf{x}) = \min\{W_k(\mathbf{x}), M_k(\mathbf{x})\}$. We consider five cases based on the optimal actions at $\mathbf{x} + \mathbf{e}_i$, \mathbf{x} , $\mathbf{x} - \mathbf{1} + \mathbf{e}_i$, and $\mathbf{x} - \mathbf{1}$, as shown in the Table EC.6. Note that the action 0 means wait at the state, and the action 1 means match at the state. Due to the monotonicity of Δ_k , other action pairs are impossible.

Table EC.6 Optimal actions at different states

State	Case 1	Case 2	Case 3	Case 4	Case 5
$\mathbf{x} + \mathbf{e}_i$	0	1	1	1	1
\mathbf{x}	0	0	1	1	1
$\mathbf{x} - \mathbf{1} + \mathbf{e}_i$	0	0	0	1	1
$\mathbf{x} - \mathbf{1}$	0	0	0	0	1

- **Case 1:** Wait at all four states.

$J_{k+1}(\mathbf{z}) = W_k(\mathbf{z})$ for $\mathbf{z} \in \{\mathbf{x} + \mathbf{e}_i, \mathbf{x}, \mathbf{x} - \mathbf{1} + \mathbf{e}_i, \mathbf{x} - \mathbf{1}\}$. Using $W_k(\mathbf{z}) = c(\mathbf{z}) + \mathcal{E}J_k(\mathbf{z})$ and $c(\mathbf{x}) - c(\mathbf{x} - \mathbf{1}) = \sum c_i$, we have:

$$G_{k+1}(\mathbf{x}) = \sum c_i + \mathcal{E}G_k(\mathbf{x}).$$

Then

$$G_{k+1}(\mathbf{x} + \mathbf{e}_i) - G_{k+1}(\mathbf{x}) = \mathcal{E}[G_k(\mathbf{x} + \mathbf{e}_i) - G_k(\mathbf{x})].$$

By the inductive hypothesis (ii) for k ,

$$G_k(\mathbf{x} + \mathbf{e}_i) - G_k(\mathbf{x}) \geq f(\mathbf{x} + \mathbf{e}_i) - f(\mathbf{x}).$$

Since f is convex and supermodular, the function $g(\mathbf{x}) = f(\mathbf{x} + \mathbf{e}_i) - f(\mathbf{x})$ is non-decreasing by Lemma EC.1. The expectation operator preserves the non-decreasing property (as it is a convex combination of shifted values). Thus,

$$\mathcal{E}[G_k(\mathbf{x} + \mathbf{e}_i) - G_k(\mathbf{x})] \geq \mathcal{E}g(\mathbf{x}) \geq g(\mathbf{x}) = f(\mathbf{x} + \mathbf{e}_i) - f(\mathbf{x}).$$

Property (ii) holds.

- **Case 2:** Only match at state $\mathbf{x} + \mathbf{e}_i$.

$J_{k+1}(\mathbf{x} + \mathbf{e}_i) = M_k(\mathbf{x} + \mathbf{e}_i)$ and $J_{k+1}(\mathbf{z}) = W_k(\mathbf{z})$ for $\mathbf{z} \in \{\mathbf{x}, \mathbf{x} - \mathbf{1} + \mathbf{e}_i, \mathbf{x} - \mathbf{1}\}$. Using (EC.3), we have:

$$G_{k+1}(\mathbf{x} + \mathbf{e}_i) = M_k(\mathbf{x} + \mathbf{e}_i) - W_k(\mathbf{x} - \mathbf{1} + \mathbf{e}_i) = f(\mathbf{x} + \mathbf{e}_i). \text{ Then}$$

$$\begin{aligned} G_{k+1}(\mathbf{x} + \mathbf{e}_i) - G_{k+1}(\mathbf{x}) &= f(\mathbf{x} + \mathbf{e}_i) - W_k(\mathbf{x}) + W_k(\mathbf{x} - \mathbf{1}) \\ &= f(\mathbf{x} + \mathbf{e}_i) - f(\mathbf{x}) + f(\mathbf{x}) - W_k(\mathbf{x}) + W_k(\mathbf{x} - \mathbf{1}) \\ &= f(\mathbf{x} + \mathbf{e}_i) - f(\mathbf{x}) + M_k(\mathbf{x}) - W_k(\mathbf{x}) \\ &\geq f(\mathbf{x} + \mathbf{e}_i) - f(\mathbf{x}), \end{aligned}$$

where the last inequality follows from the fact that at state \mathbf{x} , the optimal action is to wait, i.e., $M_k(\mathbf{x}) \geq W_k(\mathbf{x})$.

Property (ii) holds.

- **Case 3:** Match at states $\mathbf{x} + \mathbf{e}_i$ and \mathbf{x} .

$J_{k+1}(\mathbf{z}) = M_k(\mathbf{z}) = W_k(\mathbf{z} - \mathbf{1}) + f(\mathbf{z})$ for $\mathbf{z} \in \{\mathbf{x} + \mathbf{e}_i, \mathbf{x}\}$. $J_{k+1}(\mathbf{z}) = W_k(\mathbf{z})$ for $\mathbf{z} \in \{\mathbf{x} - \mathbf{1} + \mathbf{e}_i, \mathbf{x} - \mathbf{1}\}$. Using (EC.3), we have: $G_{k+1}(\mathbf{x} + \mathbf{e}_i) = M_k(\mathbf{x} + \mathbf{e}_i) - W_k(\mathbf{x} - \mathbf{1} + \mathbf{e}_i) = f(\mathbf{x} + \mathbf{e}_i)$ and similarly, $G_{k+1}(\mathbf{x}) = M_k(\mathbf{x}) - W_k(\mathbf{x} - \mathbf{1}) = f(\mathbf{x})$. Thus, $G_{k+1}(\mathbf{x} + \mathbf{e}_i) - G_{k+1}(\mathbf{x}) = f(\mathbf{x} + \mathbf{e}_i) - f(\mathbf{x})$. Property (ii) holds.

- **Case 4:** Only wait at state $\mathbf{x} - \mathbf{1}$.

$J_{k+1}(\mathbf{z}) = M_k(\mathbf{z})$ for $\mathbf{z} \in \{\mathbf{x} + \mathbf{e}_i, \mathbf{x}, \mathbf{x} - \mathbf{1} + \mathbf{e}_i\}$ and $J_{k+1}(\mathbf{x} - \mathbf{1}) = W_k(\mathbf{x} - \mathbf{1})$. Then

$$\begin{aligned}
G_{k+1}(\mathbf{x} + \mathbf{e}_i) - G_{k+1}(\mathbf{x}) &= M_k(\mathbf{x} + \mathbf{e}_i) - M_k(\mathbf{x} - \mathbf{1} + \mathbf{e}_i) - M_k(\mathbf{x}) + W_k(\mathbf{x} - \mathbf{1}) \\
&= M_k(\mathbf{x} + \mathbf{e}_i) - M_k(\mathbf{x} - \mathbf{1} + \mathbf{e}_i) - f(\mathbf{x}) \\
&= M_k(\mathbf{x} + \mathbf{e}_i) - M_k(\mathbf{x} - \mathbf{1} + \mathbf{e}_i) - f(\mathbf{x} + \mathbf{e}_i) + f(\mathbf{x} + \mathbf{e}_i) - f(\mathbf{x}) \\
&= W_k(\mathbf{x} - \mathbf{1} + \mathbf{e}_i) - M_k(\mathbf{x} - \mathbf{1} + \mathbf{e}_i) + f(\mathbf{x} + \mathbf{e}_i) - f(\mathbf{x}) \\
&\geq f(\mathbf{x} + \mathbf{e}_i) - f(\mathbf{x}),
\end{aligned}$$

where the last inequality follows from the fact that at state $\mathbf{x} - \mathbf{1} + \mathbf{e}_i$, the optimal action is to match, i.e., $M_k(\mathbf{x} - \mathbf{1} + \mathbf{e}_i) \leq W_k(\mathbf{x} - \mathbf{1} + \mathbf{e}_i)$. Property (ii) holds.

- **Case 5:** Match at all four states.

$J_{k+1}(\mathbf{z}) = M_k(\mathbf{z})$ for $\mathbf{z} \in \{\mathbf{x} + \mathbf{e}_i, \mathbf{x}, \mathbf{x} - \mathbf{1} + \mathbf{e}_i, \mathbf{x} - \mathbf{1}\}$. Using $M_k(\mathbf{z}) = f(\mathbf{z}) + c(\mathbf{z} - \mathbf{1}) + \mathcal{E}J_k(\mathbf{z} - \mathbf{1})$ and $c(\mathbf{z}) - c(\mathbf{z} - \mathbf{1}) = \sum c_i$, we have: $G_{k+1}(\mathbf{x}) = \sum c_i + f(\mathbf{x}) - f(\mathbf{x} - \mathbf{1}) + \mathcal{E}G_k(\mathbf{x} - \mathbf{1})$. Then, we have:

$$\begin{aligned}
G_{k+1}(\mathbf{x} + \mathbf{e}_i) - G_{k+1}(\mathbf{x}) &= f(\mathbf{x} + \mathbf{e}_i) - f(\mathbf{x}) - f(\mathbf{x} - \mathbf{1} + \mathbf{e}_i) + f(\mathbf{x} - \mathbf{1}) + \mathcal{E}[G_k(\mathbf{x} - \mathbf{1} + \mathbf{e}_i) - G_k(\mathbf{x} - \mathbf{1})] \\
&\geq f(\mathbf{x} + \mathbf{e}_i) - f(\mathbf{x}) - f(\mathbf{x} - \mathbf{1} + \mathbf{e}_i) + f(\mathbf{x} - \mathbf{1}) + \mathcal{E}[f(\mathbf{x} - \mathbf{1} + \mathbf{e}_i) - f(\mathbf{x} - \mathbf{1})] \\
&\geq f(\mathbf{x} + \mathbf{e}_i) - f(\mathbf{x}) - f(\mathbf{x} - \mathbf{1} + \mathbf{e}_i) + f(\mathbf{x} - \mathbf{1}) + f(\mathbf{x} - \mathbf{1} + \mathbf{e}_i) - f(\mathbf{x} - \mathbf{1}) \\
&\geq f(\mathbf{x} + \mathbf{e}_i) - f(\mathbf{x}),
\end{aligned}$$

where the second inequality follows from inductive hypothesis (ii), the third inequality follows from the fact that f is convex and supermodular and Lemma EC.1. Property (ii) holds.

Having established (ii) for $k + 1$, we prove (i) for $k + 1$.

$$\begin{aligned}
\Delta_{k+1}(\mathbf{x} + \mathbf{e}_i) - \Delta_{k+1}(\mathbf{x}) &= -(f(\mathbf{x} + \mathbf{e}_i) - f(\mathbf{x})) + \mathcal{E}[G_{k+1}(\mathbf{x} + \mathbf{e}_i) - G_{k+1}(\mathbf{x})] \\
&\geq -(f(\mathbf{x} + \mathbf{e}_i) - f(\mathbf{x})) + \mathcal{E}[f(\mathbf{x} + \mathbf{e}_i) - f(\mathbf{x})] \\
&\geq -(f(\mathbf{x} + \mathbf{e}_i) - f(\mathbf{x})) + f(\mathbf{x} + \mathbf{e}_i) - f(\mathbf{x}) \\
&= 0.
\end{aligned}$$

Thus, $\Delta_{k+1}(\mathbf{x})$ is non-decreasing, and the optimal policy is monotone for $k + 1$, the induction completes.

In our problem setting, the state space is countable, with finite action space, and the cost function is well-defined and bounded, thus the Bellman value iteration converges to optimality, i.e., $J_k(\mathbf{x}) \rightarrow J(\mathbf{x})$ and $\Delta_k(\mathbf{x}) \rightarrow \Delta(\mathbf{x})$. Therefore, we conclude that $\Delta(\mathbf{x})$ is non-decreasing, and the optimal policy is monotone in \mathbf{x} . \square

EC.2.2. Proof of Theorem 2

We prove this theorem through fluid limit analysis. The proof proceeds in four steps: (i) we define the stochastic system and its fluid scaling; (ii) we establish convergence to a deterministic fluid limit; (iii) we derive the optimal steady-state queue length; and (iv) we compute the cost ratio at optimality.

Step 1: Stochastic System and Fluid Scaling Consider a sequence of systems indexed by $n \in \mathbb{N}$, where the arrival rate scales as $\lambda_n = n\lambda$ for some base rate $\lambda > 0$. In the n -th system, let:

- $A_i^n(t)$ denote the cumulative number of type- i arrivals by time t , which is a Poisson process with rate $n\lambda/2$ for $i = 1, 2$;
- $D^n(t)$ denote the cumulative number of matches executed by time t ;
- $X_i^n(t)$ denote the number of unmatched type- i agents at time t .

The queue dynamics satisfy:

$$X_i^n(t) = X_i^n(0) + A_i^n(t) - D^n(t), \quad i = 1, 2. \quad (\text{EC.5})$$

Define the scaled processes:

$$\bar{X}_i^n(t) := \frac{X_i^n(t)}{n}, \quad \bar{A}_i^n(t) := \frac{A_i^n(t)}{n}, \quad \bar{D}^n(t) := \frac{D^n(t)}{n}.$$

Step 2: Convergence to Fluid Limit We establish that as $n \rightarrow \infty$, the scaled queue process $\bar{X}^n(t) = (\bar{X}_1^n(t), \bar{X}_2^n(t))$ converges to a deterministic fluid limit. The proof consists of three parts: (a) convergence of the arrival process, (b) tightness of the queue process, and (c) characterization of the limit.

Part (a): Convergence of Arrivals. Since $A_i^n(t)$ is a Poisson process with rate $n\lambda/2$, by the strong law of large numbers for Poisson processes, the scaled arrival process converges almost surely:

$$\bar{A}_i^n(t) = \frac{A_i^n(t)}{n} \rightarrow \frac{\lambda t}{2} \quad \text{a.s., uniformly on } [0, T],$$

for any fixed $T > 0$.

Part (b): Tightness. The scaled queue process $\{\bar{X}^n\}_{n \geq 1}$ is tight in $\mathcal{D}([0, T], \mathbb{R}^2)$ (the space of càdlàg functions with the Skorokhod J_1 topology). We verify the standard sufficient conditions: for each $i \in \{1, 2\}$,

- (i) $\sup_n \mathbb{E}[|\bar{X}_i^n(0)|] < \infty$, and
- (ii) $\lim_{\delta \rightarrow 0} \limsup_{n \rightarrow \infty} \mathbb{P}(\omega_{\bar{X}_i^n}(\delta) > \epsilon) = 0$ for every $\epsilon > 0$,

where $\omega_f(\delta) := \sup_{|s-t| \leq \delta} |f(s) - f(t)|$ is the modulus of continuity.

Condition (i) holds by assuming $X_i^n(0)/n \rightarrow \bar{X}_i(0)$ for some constant $\bar{X}_i(0) \geq 0$ (i.e., initial queues scale linearly with n).

For condition (ii), from (EC.5), we have for $s < t$:

$$|\bar{X}_i^n(t) - \bar{X}_i^n(s)| \leq |\bar{A}_i^n(t) - \bar{A}_i^n(s)| + |\bar{D}^n(t) - \bar{D}^n(s)|.$$

For the arrival increments, since $A_i^n(t) - A_i^n(s) \sim \text{Poisson}(n\lambda(t-s)/2)$:

$$\mathbb{E}[|\bar{A}_i^n(t) - \bar{A}_i^n(s)|] = \frac{\lambda(t-s)}{2}.$$

For the departure increments, since D^n is non-decreasing and each match requires one agent from each type, as our optimal policy is a threshold policy, the number of matches in $(s, t]$ is bounded by the maximum of the number of the newly arrival agents in each type queue (otherwise it has already been matched at time s):

$$D^n(t) - D^n(s) \leq \max_{j \in \{1, 2\}} \{A_j^n(t) - A_j^n(s)\}.$$

Taking expectations and using $\mathbb{E}[\max(Y_1, Y_2)] \leq \mathbb{E}[Y_1 + Y_2]$:

$$\mathbb{E}[\bar{D}^n(t) - \bar{D}^n(s)] \leq \lambda(t - s).$$

Therefore:

$$\mathbb{E}[\omega_{\bar{X}_i^n}(\delta)] \leq \frac{3}{2}\lambda\delta,$$

which implies $\lim_{\delta \rightarrow 0} \limsup_{n \rightarrow \infty} \mathbb{E}[\omega_{\bar{X}_i^n}(\delta)] = 0$. Tightness follows via Markov's inequality: for any $\epsilon, \eta > 0$, choose δ small enough that $\lambda\delta < \frac{2}{3}\epsilon\eta$, then for n large enough, $\mathbb{P}(\omega_{\bar{X}_i^n}(\delta) > \epsilon) \leq \mathbb{E}[\omega_{\bar{X}_i^n}(\delta)]/\epsilon < \eta$.

Part (c): Characterization and Uniqueness of the Limit. By tightness, any subsequence of $\{(\bar{X}^n, \bar{D}^n)\}$ has a further subsequence that converges weakly to some limit (\bar{X}, \bar{D}) . We now characterize this limit.

From the scaled dynamics $\bar{X}_i^n(t) = \bar{X}_i^n(0) + \bar{A}_i^n(t) - \bar{D}^n(t)$ and the a.s. convergence $\bar{A}_i^n(t) \rightarrow \lambda t/2$, any limit point must satisfy:

$$\bar{X}_i(t) = \bar{X}_i(0) + \frac{\lambda t}{2} - \bar{D}(t), \quad i = 1, 2. \quad (\text{EC.6})$$

Note that $\bar{D}(t)$ is monotone increasing and has bounded variation on $[0, T]$, with jumps $O(\frac{1}{n})$ vanishing as $n \rightarrow \infty$, hence absolutely continuous. Therefore, by Lebesgue's differentiation theorem, $\bar{D}(t) = \int_0^t \bar{\mu}(s) ds$ for some non-negative rate function $\bar{\mu}(s) := \frac{d\bar{D}}{ds}$, which exists almost everywhere. Physically, $\bar{\mu}(t) = 0$ whenever $\min_i \bar{X}_i(t) = 0$ (matching requires agents from both types).

Differentiating (EC.6):

$$\frac{d}{dt} \bar{X}_i(t) = \frac{\lambda}{2} - \bar{\mu}(t), \quad i = 1, 2. \quad (\text{EC.7})$$

Given initial condition $\bar{X}(0)$ and the optimal threshold policy that specifies $\bar{\mu}(t)$ as a Lipschitz function of the state $\bar{X}(t)$, the ODE (EC.7) has a unique solution by the Picard-Lindelöf theorem. By symmetry ($c_1 = c_2 = c$ and equal arrival rates $\lambda/2$), starting from symmetric initial conditions $\bar{X}_1(0) = \bar{X}_2(0)$, we have $\bar{X}_1(t) = \bar{X}_2(t)$ for all $t \geq 0$. Since the limit is uniquely determined, the entire sequence $\{(\bar{X}^n)\}_{n \geq 1}$ converges, completing the fluid limit argument.

In steady state, $\frac{d}{dt} \bar{X}_i(t) = 0$, which implies $\bar{\mu}^* = \lambda/2$. By symmetry, the optimal steady-state queue lengths satisfy $\bar{X}_1^* = \bar{X}_2^* =: \bar{X}^*$.

Step 3: Optimal Steady-State Queue Length In the fluid limit, under Assumption 2, the matching cost when both queues have length \bar{X} is:

$$f(\bar{X}, \bar{X}) = \frac{\kappa}{(\bar{X} \cdot \bar{X})^\beta} = \frac{\kappa}{\bar{X}^{2\beta}}.$$

The steady-state cost rate, comprising both waiting and matching costs, is:

$$J(\bar{X}) = \underbrace{2c\bar{X}}_{\text{waiting cost rate}} + \underbrace{\frac{\lambda}{2} \cdot \frac{\kappa}{\bar{X}^{2\beta}}}_{\text{matching cost rate}}, \quad (\text{EC.8})$$

where the matching cost rate equals the matching rate ($\lambda/2$) times the cost per match.

To find the optimal queue length, we minimize $J(\bar{X})$ over $\bar{X} > 0$. Taking the derivative and setting it to zero:

$$\frac{dJ}{d\bar{X}} = 2c - 2\beta \cdot \frac{\lambda\kappa}{2\bar{X}^{2\beta+1}} = 2c - \frac{\beta\lambda\kappa}{\bar{X}^{2\beta+1}} = 0.$$

Solving for \bar{X} :

$$\bar{X}^{2\beta+1} = \frac{\beta\lambda\kappa}{2c} \implies \bar{X}^* = \left(\frac{\beta\lambda\kappa}{2c}\right)^{\frac{1}{2\beta+1}}. \quad (\text{EC.9})$$

The second derivative $\frac{d^2J}{d\bar{X}^2} = (2\beta)(2\beta+1) \frac{\lambda\kappa}{2\bar{X}^{2\beta+2}} > 0$ confirms this is a minimum.

Step 4: Cost Ratio at Optimality At the optimal steady state \bar{X}^* , we compute the waiting and matching cost rates separately.

Waiting cost rate:

$$W^* = 2c\bar{X}^* = 2c \left(\frac{\beta\lambda\kappa}{2c}\right)^{\frac{1}{2\beta+1}}.$$

Matching cost rate:

$$M^* = \frac{\lambda}{2} \cdot \frac{\kappa}{(\bar{X}^*)^{2\beta}} = \frac{\lambda\kappa}{2} \left(\frac{2c}{\beta\lambda\kappa}\right)^{\frac{2\beta}{2\beta+1}}.$$

Using the optimality condition (EC.9), we have $(\bar{X}^*)^{2\beta+1} = \frac{\beta\lambda\kappa}{2c}$, which gives:

$$(\bar{X}^*)^{2\beta} = \frac{(\bar{X}^*)^{2\beta+1}}{\bar{X}^*} = \frac{\beta\lambda\kappa}{2c\bar{X}^*}.$$

Substituting into the matching cost rate:

$$M^* = \frac{\lambda\kappa}{2} \cdot \frac{2c\bar{X}^*}{\beta\lambda\kappa} = \frac{c\bar{X}^*}{\beta}.$$

Therefore, the ratio of waiting to matching costs is:

$$\frac{W^*}{M^*} = \frac{2c\bar{X}^*}{\frac{c\bar{X}^*}{\beta}} = 2\beta. \quad (\text{EC.10})$$

□